

MegaLMM: Mega-scale linear mixed models for genomic predictions with thousands of traits

Daniel E Runcie¹, Jiayi Qu², Hao Cheng³ and Lorin Crawford⁴

¹Department of Plant Sciences, University of California Davis, Davis, CA, USA; deruncie@ucdavis.edu, ²Department of Animal Sciences, University of California Davis, Davis, CA, USA; jyqq@ucdavis.edu, ³Department of Animal Sciences, University of California Davis, Davis, CA, USA; qtlcheng@ucdavis.edu, ⁴Microsoft Research New England, Cambridge, MA, USA; lcrawford@microsoft.com

ABSTRACT Large-scale phenotype data can enhance the power of genomic prediction in plant and animal breeding, as well as human genetics. However, the statistical foundation of multi-trait genomic prediction is based on the multivariate linear mixed effect model, a tool notorious for its fragility when applied to more than a handful of traits. We present MegaLMM, a statistical framework and associated software package for mixed model analyses of a virtually unlimited number of traits. Using three examples with real plant data, we show that MegaLMM can leverage thousands of traits at once to significantly improve genetic value prediction accuracy.

KEYWORDS Multi-trait Linear Mixed Model, Genomic prediction, High-throughput phenotyping, Multi-environment trial

1

2 Background

3 New high-throughput phenotyping technologies hold promise
4 for a revolution in data-driven decisions in plant and animal
5 breeding programs (Araus *et al.* 2018; Koltes *et al.* 2019). For
6 example, drone-based hyperspectral cameras can image fields
7 at high resolution across hundreds of spectral bands (Rutkoski
8 *et al.* 2016), wearable sensors can continuously monitor animals
9 health and physiology (Neethirajan 2017), and RNA sequencing
10 and metabolite profiling can simultaneously assay the concentrations
11 of tens-of-thousands of targets (Schrag *et al.* 2018). These
12 high-dimensional traits could allow breeders to rapidly assess
13 many aspects of performance more accurately or earlier in development
14 than was possible using traditional tools. This can increase the rate of gain in target traits by increasing selection
15 accuracy, increasing selection intensity, and reducing breeding
16 cycle durations.

17 However, efficiently incorporating high-dimensional phenotype data into breeding decisions is challenging. Whenever two
18 traits are genetically correlated, joint analyses can improve the
19 precision of variety evaluation (Thompson and Meyer 1986).
20 However, two key problems emerge. First, the number of traits in high-dimensional datasets is often much larger than the number of breeding lines, which means that naive correlation estimates are not robust. Second, phenotypic correlation among traits are often poor approximations to genetic correlation, so not all correlated traits are useful for breeding decisions (Bernardo 2010). For example, plants grown in more productive areas of a field will tend to produce higher yields and be greener (measured by hyperspectral reflectance). Yet, selecting indirectly based on green plants instead of directly on higher yields may be counter-productive because “green-ess” may indicate an over-investment in vegetative tissues at the expense of seed. This contrasts with the problem of predicting genetic values

35 from genotype data (e.g., genomic prediction; Meuwissen *et al.*
36 (2001)), where all correlations between candidate features and
37 performance are useful for selection.

38 The multivariate linear mixed model (MvLMM) is a widely-used
39 statistical tool for decomposing phenotypic correlations into genetic and non-genetic components. The MvLMM is a
40 multi-outcome generalization of the univariate linear mixed
41 model (LMM) that forms the backbone of the majority of methods in quantitative genetics. The MvLMM was introduced over
42 40 years ago (Henderson and Quaas 1976), and has repeatedly
43 been shown to increase selection efficiency (Piepho *et al.* 2007;
44 Calus and Veerkamp 2011; Jia and Jannink 2012). Yet, MvLMMs
45 are still rarely used in actual breeding programs because naive
46 implementations of the framework are sensitive to noise, prone
47 to overfitting, and exhibit convergence problems (Johnstone
48 and Titterington 2009). Furthermore, existing algorithms are
49 extremely computationally demanding. The fragility of naive
50 MvLMMs is due to the number of variance-covariance parameters
51 that must be estimated which increases quadratically with the
52 number of traits. The computational demands increase even
53 more dramatically: from cubically to quintically with the number
54 of traits (Zhou and Stephens 2014) because most algorithms
55 require repeated inversion of large covariance matrices. These
56 matrix operations dominate the time required to fit a MvLMMs,
57 leading to models that take days, weeks, or even years to converge.

58 Here, we describe MegaLMM (linear mixed models for millions
59 of observations), a novel statistical method and computational
60 algorithm for fitting massive-scale MvLMMs to large-scale phenotypic
61 datasets. Although we focus on plant breeding applications for concreteness, our method can be broadly applied
62 wherever multi-trait linear mixed models are used (e.g., human
63 genetics, industrial experiments, psychology, linguistics, etc.).
64 MegaLMM dramatically improves upon existing methods
65 that fit low-rank MvLMMs, allowing multiple random effects
66 and un-balanced study designs with large amounts of missing
67 data. We achieve both scalability and statistical robustness by

¹ Dept. of Plant Sciences, University of California, Davis, CA, USA E-mail:
deruncie@ucdavis.edu

72 combining strong, but biologically motivated, Bayesian priors
73 for statistical regularization—analogous to the $p >> n$ approach
74 of genomic prediction methods—with algorithmic innovations
75 recently developed for LMMs. In the three examples below, we
76 demonstrate that our algorithm maintains high predictive accu-
77 racy for tens-of-thousands of traits, and dramatically improves
78 the prediction of genetic values over existing methods when
79 applied to data from real breeding programs.

80 Results

81 Methods overview.

82 MegaLMM fits a full multi-trait linear mixed model (MvLMM)
83 to a matrix of phenotypic observations for n genotypes and
84 t traits (level 1 of Figure 1A). We decompose this matrix into
85 fixed, random, and residual components, while modeling the
86 sources of variation and covariation among all pairs of traits.
87 The main statistical and computational challenge of fitting large
88 MvLMMs centers around the need to robustly estimate $t \times t$
89 covariance matrices for the residuals and each random effect.
90 Each covariance matrix has $t(t-1)/2 + t$ free parameters, and
91 any direct estimation approach is computationally demanding
92 because it requires repeatedly inverting these matrices (an $\mathcal{O}(t^3)$
93 operation).

94 We solve both of these problems by introducing K un-
95 observed (latent) traits called factors (\mathbf{f}_k) to represent the causes
96 of covariance among the t observed traits. We treat each latent
97 trait just as we would any directly measured trait and decom-
98 pose its variation into the same fixed, random and residual com-
99 ponents using a set of parallel univariate linear mixed models
100 (level 2 of Figure 1A). We then model the pairwise correlations
101 between each latent trait and each observed trait through K
102 loadings vectors λ_k .

103 Together, the set of parallel univariate LMMs and the set
104 of factor loading vectors result in a novel and very general re-
105 parameterization of the MvLMM framework as a mixed-effect
106 factor model. This parameterization leads to dramatic computa-
107 tional performance gains by avoiding all large matrix inversions.
108 It also serves as a scaffold for eliciting Bayesian priors that are
109 intuitive and provide powerful regularization which is neces-
110 sary for robust performance with limited data. Our default prior
111 distributions encourage: i) shrinkage on the factor-trait corre-
112 lations (λ_{jk}) to avoid over-fitting covariances, and ii) shrinkage on
113 the factor sizes to avoid including too many latent traits. This
114 two-dimensional regularization helps the model focus only on
115 the strongest, most relevant signals in the data.

116 While others have used latent factor approaches to reduce
117 dimensionality of MvLMMs (e.g., [de Los Campos and Gianola 2007](#);
118 [Meyer 2007](#); [Runcie and Mukherjee 2013](#); [Dahl et al. 2016](#)),
119 these methods only use factors for a single random effect (usu-
120 ally the matrix of random genetic values)—with the exception
121 of BSFG which uses factors for the combined effect of a single
122 random effect and the residuals ([Runcie and Mukherjee 2013](#)).
123 In MegaLMM, we expand this framework and use factors to model
124 the joint effects of all predictors: fixed, random and residual
125 factors on multiple traits.

126 We combine this efficient factor model structure with algo-
127 rithmic innovations that greatly enhance computational efficiency,
128 drawing upon recent work in LMMs ([Kang et al. 2008](#); [Zhou and Stephens 2012](#);
129 [Lippert et al. 2011](#); [Runcie and Crawford 2019](#)). While Gibbs samplers for MvLMMs are notoriously slow,
130 we discovered extensive opportunities for collapsing sampling

132 steps, marginalizing over missing data, and discritizing vari-
133 ance components so that intermediate results can be cached
134 (Supplemental Methods).

135 Genomic prediction using MegaLMM works by fitting the
136 model to a partially observed trait matrix, with the traits to
137 be predicted imputed as missing data. MegaLMM then estimates
138 genetic values for all traits (both observed and missing) in a
139 single step (Figure 1B).

140 **MegaLMM is efficient and effective for large datasets**

141 We used a gene expression matrix with 20,843 genes measured
142 in each of 665 *Arabidopsis thaliana* accessions (a total of nearly 14
143 million observations), to evaluate the accuracy and time require-
144 ments for trait-assisted genomic prediction—a classic example
145 of an applied use of MvLMMs—across a panel of existing soft-
146 ware packages. We created datasets with 4 to 20,842 “secondary”
147 traits with complete data, and used these data to predict the
148 genetic values of a single randomly selected “focal” gene with
149 50% missing data.

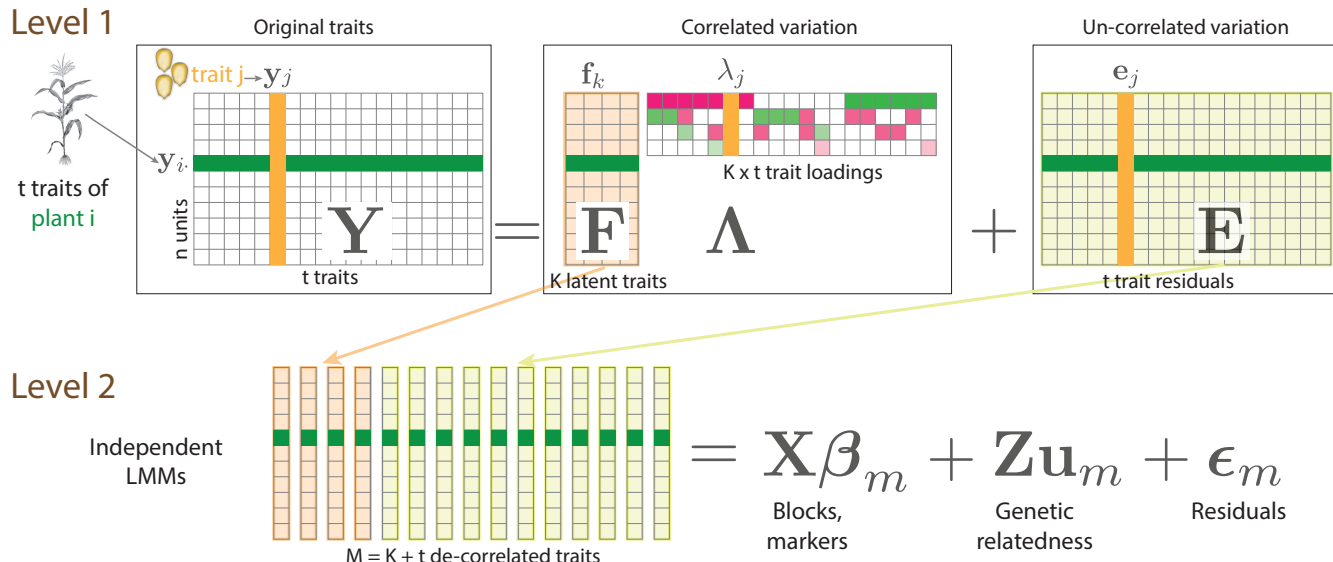
150 Despite the limited number of independent lines in this data
151 set, adding up to ≈ 200 secondary traits improved the genomic
152 prediction accuracy of MegaLMM and two other Bayesian meth-
153 ods: MCMCglmm and phenix (Figure 2A). The maximum likeli-
154 hood method MTG2 ([Lee and van der Werf 2016](#)), on the other
155 hand, did only marginally better than single-trait prediction,
156 and genomic prediction accuracy declined with 32 traits, likely
157 due to overfitting. We note that the results here are averages
158 over 20 randomly selected focal genes. The prediction accuracy
159 and benefits of multi-trait prediction varied considerably among
160 genes (Figures S1 and S2), but comparisons among methods
161 were largely correlated. Using simulated datasets where we
162 knew the true genetic and residual covariances among traits, we
163 also found that MegaLMM was at least as accurate in estimating
164 covariance parameters as the competing methods (Figure S3).

165 Beyond 32 secondary traits, computational times for
166 MCMCglmm and MTG2 became prohibitive (Figure 2B). Using ex-
167 trapolation, we estimated that fitting these methods for 512 traits
168 would take 20 days and 217 days, respectively, without consid-
169 ering issues of model convergence. In contrast, phenix and
170 MegaLMM were both able to converge on good model fits for 512
171 traits in approximately one hour.

172 Beyond 512 traits, MegaLMM was the only viable method as
173 phenix cannot be applied to datasets with $t > n$ phenotypes.
174 Although the genomic prediction accuracy of MegaLMM did not
175 increase further after ≈ 256 traits, performance did not suffer
176 even with the full dataset of $> 20,000$ traits and the analysis
177 was completed in less than a day. This shows that MegaLMM
178 is feasible to apply to very high-dimensional studies and, in
179 most cases, does not require pre-filtering of traits—something
180 that requires great care in genomic prediction applications to
181 avoid misleading results ([Runcie and Cheng 2019](#)).

182 An important feature of MegaLMM is that the choice of the num-
183 ber of latent factors K is less critical than in most factor models.
184 Since factors are ordered from most-to-least important by the
185 prior (See Methods), as long as enough factors are specified to
186 capture the majority of the covariance among traits, adding ad-
187 ditional latent factors does not lead to over-fitting (Figure S4A).
188 Additional factors do increase the run-time of the algorithm,
189 though (Figure S4B), so some optimization of K during the burn-
190 in period can reduce computational demands during posterior
191 sampling.

A MegaLMM model



B Genomic Prediction applications

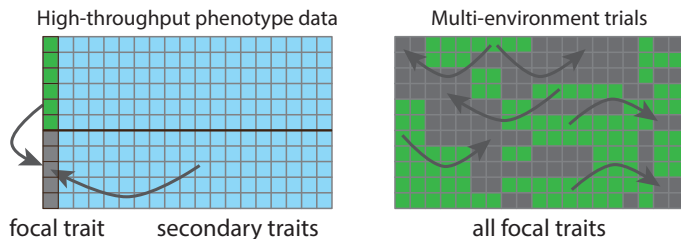


Figure 1 Overview of the MegaLMM model: A. MegaLMM decomposes a typical MvLMM into a two-level hierarchical model. In level 1, raw data from t traits on each of the n plants (more generally observational units) ($y_{i \cdot}$) are combined into an $n \times t$ trait matrix \mathbf{Y} . Variation in \mathbf{Y} is decomposed into two parts: a low-rank model ($\mathbf{F}\Lambda$) consisting of K latent factor traits, each of which controls variation in a subset of the original traits through the loadings matrix Λ , and a residual matrix (\mathbf{E}) of independent residuals for each trait. The latent factor traits and the t residual vectors are now mutually un-correlated, and are each modeled with independent LMMs in level 2. Experimental design factors, genetic background effects, and other modeling terms are introduced at this level. Cells highlighted in green show observations and associated parameters for plant i . Cells highlighted in orange highlight observations and associated parameters for trait j . B. Two multi-trait genomic prediction applications: i) the use of high-throughput phenotyping data to supplement for expensive direct measures of focal traits like grain yield, and ii) the analysis of large multi-environment trials. In each case, observed data of focal traits (green) and secondary traits (blue) are used to predict genetic values for individuals without direct phenotypic observations (grey).

192 Applications to real breeding programs

193 To demonstrate the utility of MegaLMM, we developed two classes
 194 of genomic prediction models for high-dimensional phenotype
 195 data in real plant breeding programs.

196 Genomic prediction using hyperspectral reflectance data

197 When the final performance of a variety is difficult or costly
 198 to obtain, breeding programs can supplement direct measures
 199 of performance with data from surrogate traits that can be mea-
 200 sured cheaply, earlier in the breeding cycle, and on more vari-
 201 eties. For example, in the bread wheat breeding program at CIM-
 202 MYT, hyperspectral reflectance data can be collected rapidly and
 203 repeatedly by aerial drones on thousands of plots (Krause *et al.*
 204 2019). We developed a multi-trait genomic prediction model
 205 to incorporate 62-band hyperspectral reflectance data from 10
 206 different drone flights over the course of one growing season,
 207 and compared the accuracy of these genetic value predictions

208 against more traditional approaches.

209 We first compared three standard univariate methods: GBLUP
 210 (Hayes *et al.* 2009), Bayesian LASSO (BL) (Park and Casella
 211 2013), and Reproducing kernel Hilbert space (RKHS) regression
 212 (de Los Campos *et al.* 2010). GBLUP achieved a prediction accu-
 213 racy of $\rho_g = 0.43$ for yield (Figure 3A). Both the BL and RKHS
 214 methods showed modest improvements, with $\rho_g = 0.47$ and
 215 $\rho_g = 0.49$, respectively in these data. The RKHS model often out-
 216 performs GBLUP in plant breeding datasets, but improvements
 217 are generally slight and inconsistent depending on the genetic
 218 architecture of the targeted trait.

219 In the original analysis of this dataset, Krause *et al.* (2019)
 220 achieved increased performance by replacing the genomic ker-
 221 nel (\mathbf{K} in our notation) with a kernel based on the cross-product
 222 of hyperspectral reflectances across all wavelengths and time
 223 points (termed the \mathbf{H} matrix). We replicated these results, achiev-
 224 ing a prediction accuracy of $\rho_g = 0.58$ (HBLUP method). These

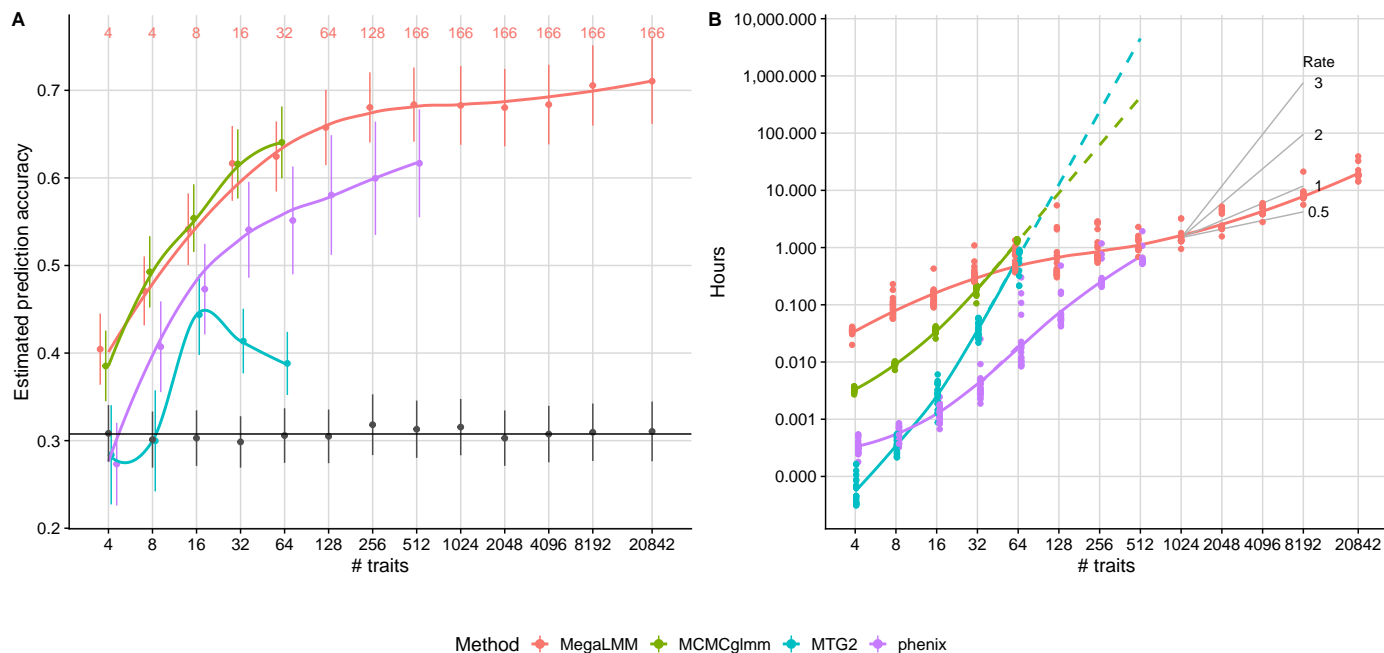


Figure 2 **MegaLMM scales efficiently for very high-dimensional traits.** Four competing methods were used to fit multi-trait genomic prediction models to predict genetic values for a single focal gene expression trait using complete data from t additional traits. Data are from an *Arabidopsis thaliana* gene expression data with 20,843 genes and 665 lines. **A)** Average estimated genomic prediction accuracy across 20 focal traits using t additional secondary traits for each of the four prediction methods (the horizontal line is the average univariate prediction accuracy). Genomic prediction accuracy was estimated by cross-validation as $\rho_g = \text{corg}_g(\hat{\mathbf{u}}, \mathbf{y}) \sqrt{h^2(\hat{\mathbf{u}})}$ to account for non-genetic correlations between the secondary traits and focal traits since all were measured in the same sample. Smoothed curves are estimated by `stats::lowess`. The number of latent factors used for MegaLMM (K) is listed in red at the top of the figure. **B)** Computational times required to find a solution for each MvLMM. For the MCMC methods MCMCglmm and MegaLMM, times were estimated as the time required to collect an effective sample size of at least 1000 for $> 90\%$ of the elements in the genetic covariance matrix \mathbf{U} . Computational times for MCMCglmm and MTG2 above 64 traits were linearly extrapolated (on log scale) based on the slope between 32 and 64 traits. Black lines show the slope of exponential scaling functions with the specified exponents for reference.

225 authors also proposed a multi-kernel model combining the \mathbf{K} 250 and \mathbf{H} kernel matrices, although they only applied this to cross- 226 treatment genotype-by-environment predictions. We found that 227 applying this multi-kernel method to the within-environment 228 data resulted in additional accuracy gains ($\rho_g = 0.64$) (GBLUP+H 229 method; Figure 3A).

230 While more effective than univariate methods, predictions 231 based on the \mathbf{H} kernel matrix are biased by non-genetic cor- 232 relations between surrogate traits and yield because they do 233 not directly model the genetic component of these correlations. 234 MegaLMM implements a full multi-trait mixed model and thus 235 can separate these sources of correlation. We fit three differ- 236 ent multi-trait prediction models with MegaLMM. The first was 237 a standard multi-trait mixed model with a single random ef- 238 fect based on the genomic relationship matrix \mathbf{K} . This method 239 achieved a dramatically higher prediction accuracy than any of 240 the previous approaches ($\rho_g = 0.73$). Second, because the RKHS 241 model had the highest performance among univariate predic- 242 tions, we implemented an approximate RKHS method in MegaLMM 243 based on averaging over three kernel matrices (de Los Campos 244 *et al.* 2010). We are not aware of any other high-dimensional 245 MvLMM implementations that allow models with multiple ran- 246 dom effects. This model achieved the highest predictive ac- 247 curacy ($\rho_g = 0.77$). Finally, we repeated the MegaLMM-GBLUP 248 analysis but this time masking all phenotype data (both grain 249

250 yield and hyperspectral data) from the testing set. We called 251 this approach MegaLMM-GBLUP-CV1 following the nomenclature 252 from Burgueño *et al.* (2012). Genetic prediction accuracy in the 253 CV1 setting was similar to the univariate methods ($\rho_g = 0.49$), 254 showing that nearly all benefit of MegaLMM in this dataset came 255 through the optimal use of secondary trait phenotypes on the 256 lines of interest.

257 In summary, by directly modeling the genetic covariance be- 258 between the surrogate traits (hyperspectral reflectance measures), 259 we achieved performance increases of 56%-79%, and up to 36% 260 over the HBLUP method. To show that these conclusions were 261 robust in other datasets, we repeated the same analyses in the 262 other 19 trials reported by Krause *et al.* (2019) and results were 263 highly similar in all trials (Figure S5).

264 To explore *why* directly modeling the genetic correlation is 265 important, we compared the estimated genetic correlations be- 266 between each hyperspectral band and grain yield to the corre- 267 sponding phenotypic correlations (Figure 3B). Most genetic cor- 268 relation estimates closely paralleled the phenotypic correlations, 269 with the largest values for low-to-intermediate wavelengths oc- 270 ccurring on dates towards the end of the growing season while 271 plants were in the grain filling stage (Krause *et al.* 2019). How- 272 ever, there were notable differences. For example, genomic cor- 273 relations were moderate ($\rho_g \approx 0.2$) for most wavelengths during 274 early February sampling dates while phenotypic correlations

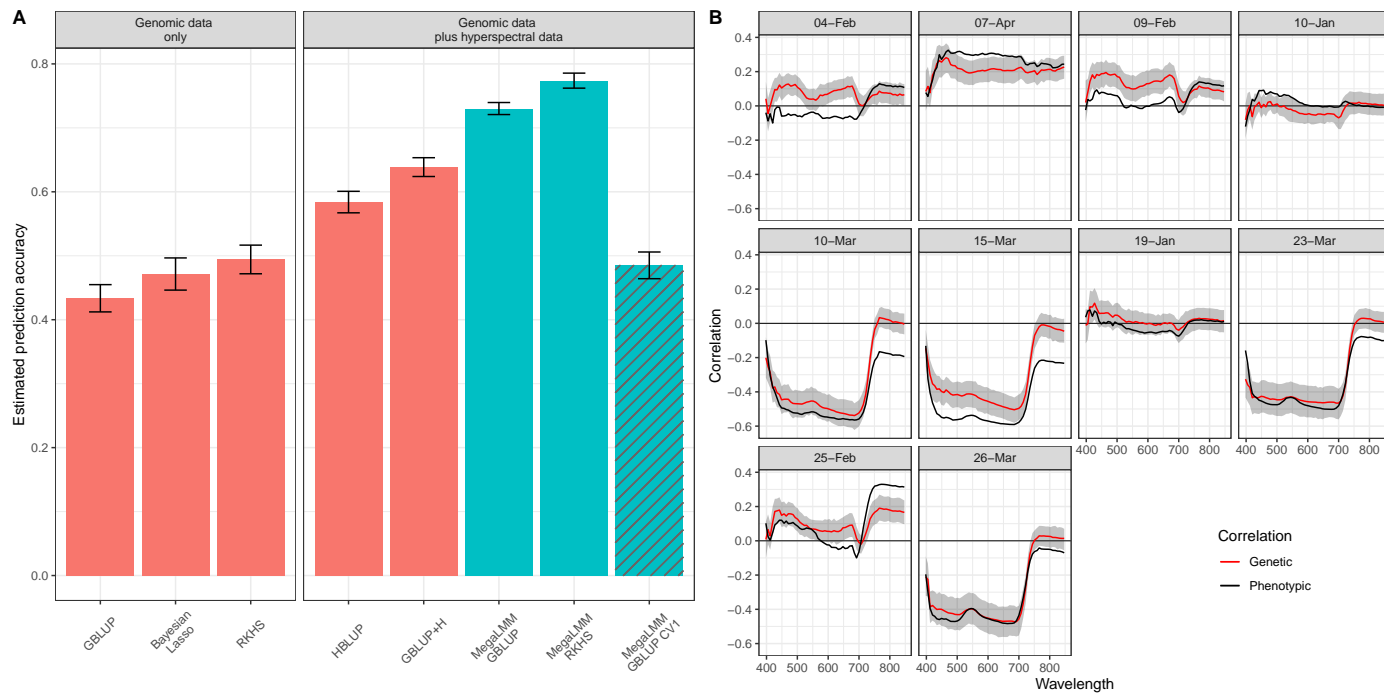


Figure 3 Performance of single-trait and multi-trait genomic prediction for wheat yield. A) 8 methods for predicting Grain Yields of 1,092 bread wheat lines. Genetic value prediction accuracy was estimated by cross-validation. Complete data (yield, marker genotypes, and 620 hyperspectral wavelength reflectances) was available for all lines, but 50% of the yield values were masked during model training. Genetic value prediction accuracy was estimated as $\rho_g = \text{cor}_g(\hat{\mathbf{u}}, \mathbf{y}) \sqrt{h^2(\hat{\mathbf{u}})}$ because hyperspectral data and actual yields were collected on the same plots (Runcie and Cheng 2019). Bars show average estimates (\pm standard error) over 20 replicate cross-validation runs for each method. Details of each model are presented in the Supplemental Methods. Briefly, the three single-trait methods only used yield and genotype data. The five multi-trait methods additionally used hyperspectral data measured on all 1,092 lines. **B)** Phenotypic correlation (black lines), and estimates of genetic correlation (red lines) between each hyperspectral wavelength measured on each of the 10 flight dates with final grain yield. Genetic correlations were estimated with the MegaLMM GBLUP method using complete data. Ribbons show the 95% highest posterior density (HPD) intervals.

were near zero; yet, during early March time points, phenotypic correlations between yield and bands around 800 nanometers were moderate ($\rho_y \approx -0.2$) but genomic correlations were near-zero. MegaLMM is able to model the discrepancy between genomic and phenotypic correlations, but methods based on the \mathbf{H} matrix (e.g., HBLUP) are not.

281 Genomic prediction of agronomic traits across multi- 282 environmental trials

283 Multi-trait mixed models are also used to analyze data from
284 multi-environment trials to account for genotype-environment
285 interactions and select the best genotypes in each environment.
286 The Genomes2Field initiative (<https://www.genomes2fields.org/>) is
287 an ongoing multi-environment field experiment of maize hybrid
288 genotypes across 20 American states and Canadian provinces.
289 Data from the years 2014-2017 included 119 trials with a total
290 of 2102 hybrids. As in many large-scale multi-environment
291 trials, only a small proportion of the available genotypes were
292 grown in each trial. Therefore, the majority of trial-genotype
293 combinations were un-observed.

294 We selected four representative agronomically important
295 traits and compared the ability of four modeling approaches
296 to impute the missing measurements. Including across-trial in-
297 formation was beneficial for each of the four traits, suggesting
298 generally positive genetic correlations across trials. However,
299 applying MegaLMM to each of the four trait datasets improved

300 predictions dramatically, with average benefits across trials rang-
301 ing from $\rho_y = 0.10$ to $\rho_y = 0.17$ (Figure 4). The performance of
302 phenix was inconsistent across traits and trials, likely because its
303 model for the non-additive genetic covariance (i.e., the residual)
304 is less flexible than MegaLMM.

305 To explore *why* jointly modeling all genetic and non-genetic
306 covariances for each pair of traits improved prediction accu-
307 racy for each trait, we assessed the per-trial differences in per-
308 formance between MegaLMM and the corresponding within-trial
309 genomic prediction model. Trials varied considerably in how
310 much MegaLMM improved genomic prediction accuracy, with sev-
311 eral trials seeing improvements of $\rho > 0.4$. The magnitude of
312 the MegaLMM effect on genomic prediction accuracy was largely
313 explained by the maximum genetic covariance between that trial
314 and any other trial in the dataset (Figure S6). This is expected
315 because the benefit of a MvLMM is largely dependent on the
316 magnitude of genetic covariances between traits.

317 A common approach in multi-environment trials is to com-
318 bine similar trials (based on geographic location or similar en-
319 vironments) into clusters and make genetic value predictions
320 separately for each cluster (Piepho and Möhring 2005). How-
321 ever, this will not be successful if clusters cannot be selected *a*
322 *priori* because using the trial data itself to identify clusters can
323 lead to overfitting if not performed carefully (Runcie and Cheng
324 2019). In these data, the distribution of genomic correlations be-
325 tween trials differed among traits, so it is not straightforward to

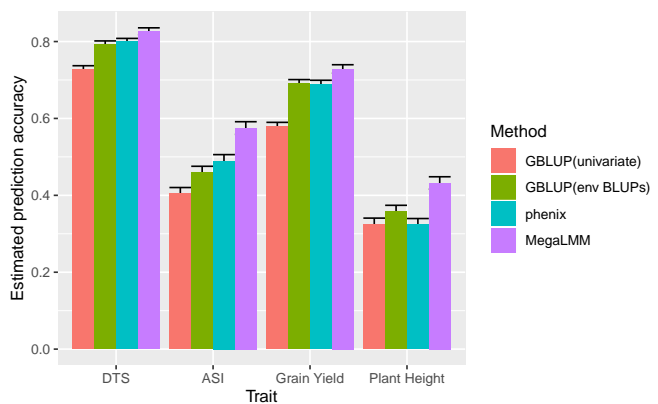


Figure 4 Average within-trial prediction accuracy for four maize traits in the Genomes2Fields Initiative experiment. Traits included: days to silking (DTS), anthesis-silking interval (ASI), grain yield, and plant height. Bars show the average $\pm 95\%$ confidence intervals of prediction accuracy for each method across the 76-99 trials with sufficient training data for each trait. For each trait, prediction accuracies were estimated as the mean over 20 randomized cross-validation replicates.

326 identify which pairs or subsets of trials could be combined. The
327 most obvious predictor of trial similarity is geographic distance,
328 but we did not see consistent spatial patterns in the among-trial
329 covariances across the four traits. The trials with the greatest
330 benefit from our MvLMM showed geographic clustering in the
331 central mid-west for the anthesis-silking interval (ASI) but not
332 for the other three traits (Figure 5A). Genetic correlations tended
333 to decrease over long distances for ASI and over short distances
334 for plant height, but not for the other two traits (Figure 5B), re-
335 sulting in obvious geographic clustering of genetic correlations
336 for ASI but not the other traits (Figure 5C). This suggests that in-
337 cluding all trials together in one model is necessary to maximize
338 the benefit of the MvLMM approach to multi-environment plant
339 breeding.

340 Discussion

341 Novel statistical methods can help optimize plant and animal
342 breeding programs to meet future food security needs. In the
343 above examples, we highlighted two areas where large-scale
344 phenotype data can improve the accuracy of genomic predic-
345 tion in realistic plant breeding scenarios: by incorporating high-
346 throughput phenotyping data from remote sensors, and by syn-
347 thetizing data on gene-environment interactions across large-
348 scale multi-environment trials. In both examples, we apply
349 high-dimensional multivariate linear mixed models to efficiently
350 integrate all available genotype and phenotype data into genetic
351 value predictions. MegaLMM is a scalable tool that extends the
352 feasible range of input data for multivariate linear mixed models
353 by at least two orders of magnitude over existing methods, while
354 providing the flexibility to plug directly into existing breeding
355 programs.

356 Computational and statistical efficiency

357 Computational issues in single-trait LMMs have been studied
358 extensively, allowing implementations for large datasets (Lip-
359 pert *et al.* 2011; Zhou and Stephens 2014; Loh *et al.* 2015; Runcie
360 and Crawford 2019). Most of these algorithms diagonalize the

361 genomic relationship matrices to improve computational effi-
362 ciency. This technique dramatically improves the performance
363 of simple, low-dimensional MvLMMs as well (e.g., Zhou and
364 Stephens 2014; Lee and van der Werf 2016). However, diagonal-
365 ization does not address the computational challenge imposed
366 by large trait-covariance matrices, and can only be applied to
367 models with a single random effect and no missing data. There-
368 fore, these tools cannot be applied to the datasets studied here or,
369 more generally, to most large-scale studies of gene-environment
370 interactions that frequently have large proportions of missing
371 data (Piepho *et al.* 2007) (Figure 1) and to studies that have exper-
372 imental designs with multiple sources of covariance (e.g., spatial
373 environmental variation or non-additive genetics).

374 Our work builds on the factor-analytic approach to regularizing
375 MvLMMs (de Los Campos and Gianola 2007; Meyer 2007;
376 Runcie and Mukherjee 2013; Dahl *et al.* 2016) and is most similar
377 to BSFG (Runcie and Mukherjee 2013) and phenix (Dahl *et al.*
378 2016), which improve upon traditional quantitative genetic fac-
379 tor models by specifying sparse or low-rank factor matrices to
380 improve robustness in high dimensions. Importantly, however,
381 these models are limited to a single random effect and are not
382 tractable for datasets with large numbers of traits because of com-
383 putational inefficiencies (BSFG), or a lack of strong regularization
384 on the residual covariance matrix (phenix). MegaLMM generalizes
385 both methods and dramatically improves their weaknesses, al-
386 lowing analyses with >20,000 traits to be completed in less than
387 one day. Since MegaLMM scales approximately linearly with the
388 number of traits (Figure 2), applying it to datasets with many
389 more traits may be feasible. While we have designed many of
390 our routines to take advantage of multi-core CPUs, graphical
391 processing units may offer additional performance gains.

392 Two key advantages of MegaLMM are its flexibility and gen-
393 erality. We have designed the MegaLMM R package to be as general
394 as possible so that it can be applied to a wide array of prob-
395 lems in quantitative genetics. MegaLMM tolerates unbalanced
396 designs with incomplete observations (something that makes
397 MCMCg1mm and MTG2 very slow), arbitrarily complex fixed effect
398 specifications to model experimental blocks, covariates, or other
399 sources of variation among samples (unlike phenix), and most
400 importantly, multiple random effects (unlike phenix, GEMMA, or
401 MTG2). Multiple random effect terms can be used to account
402 for spatially correlated variation across fields, non-additive ge-
403 netic variation that is not useful for breeding, or to more flexibly
404 model non-linear genetic architectures as we demonstrated with
405 the approximate RKHS regression approach in the wheat ap-
406 plication (Figure 3). To make multiple-random-effect models
407 computationally efficient, we take our earlier work with LMMs
408 (Runcie and Crawford 2019) and extend the same discrete estima-
409 tion procedure to MvLMMs where the impact on computational
410 efficiency is exponentially greater. Other commonly used tools
411 for fitting MvLMMs such as ASREML (Gilmour 2007) allow more
412 flexibility in the specification of multiple variance-component
413 models with correlated random effects that are not currently pos-
414 sible in MegaLMM. However, these tools do not scale well beyond
415 ≈ 10 traits, so are not feasible to apply directly to large-scale
416 datasets in plant breeding.

356 Applicability to high-throughput phenotypic data

357 Large-scale phenotype data collection is rapidly emerging as a
358 standard tool in plant breeding and other fields that use quanti-
359 tative genetics (GTEx Consortium 2017; Araus *et al.* 2018; Bycroft
360 *et al.* 2018). These deep phenotyping datasets can be used as

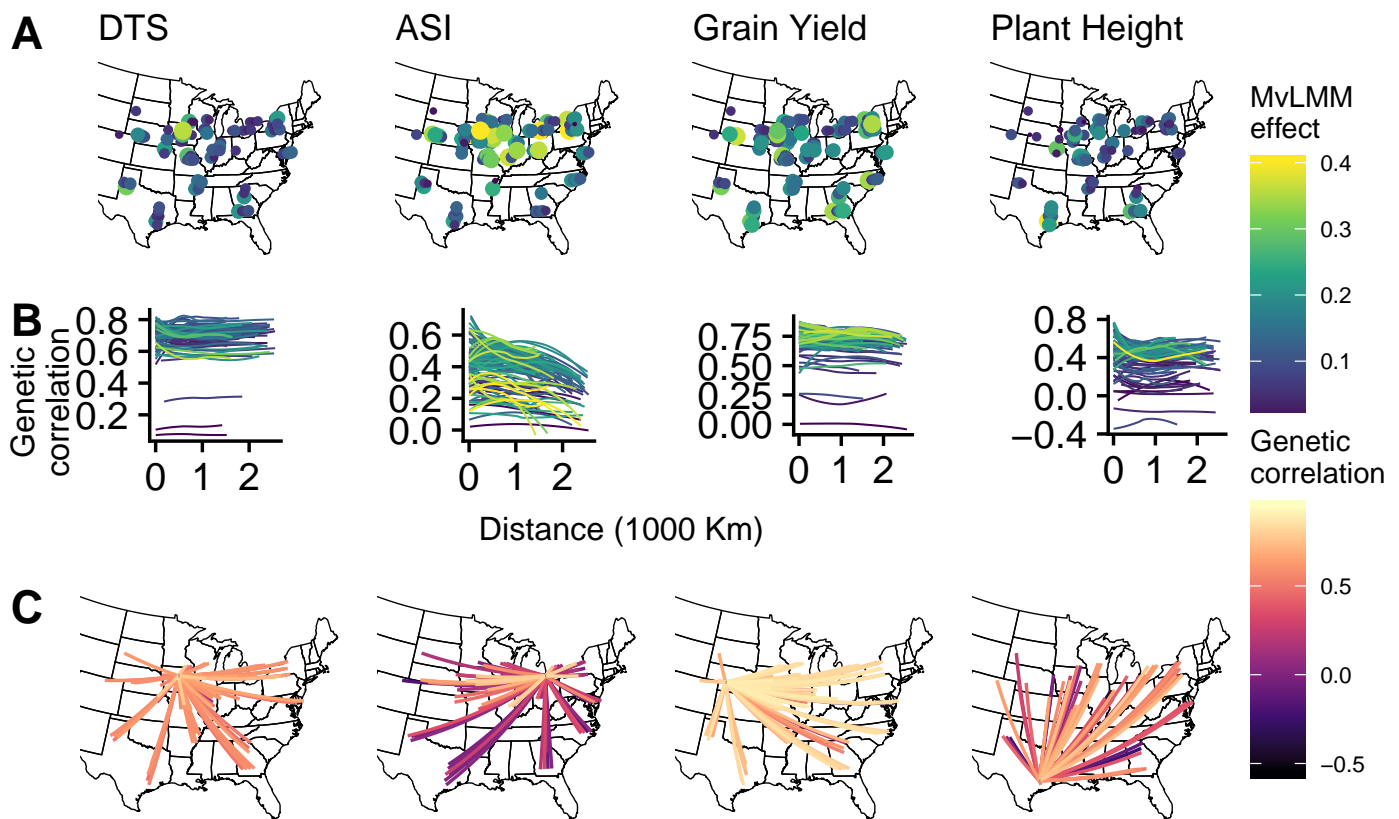


Figure 5 Benefit of *MegaLMM* and geographic distributions of among-trial genetic correlations vary among traits. Traits analyzed included: days to silking (DTS), anthesis-silking interval (ASI), grain yield, and plant height. **A)** Trial locations for each trait are shown. Points were jittered west-to-east to prevent overlap of repeated trials across years. Size and color of each point correspond to the increase in prediction accuracy for *MegaLMM* versus a univariate LMM. **B)** Smoothed estimates (computed using `geom_smooth` with a bandwidth of 1.0) of the relationship between geographic distance and genetic correlation for each trial. Line colors correspond to the benefit of *MegaLMM* in each focal trial. **C)** Genetic correlations between the trial with the greatest benefit of *MegaLMM* for each trait and each other trial.

422 high-dimensional features to predict genetic values in agronomically important traits and serve as substitutes for direct assays
423 where these are more time-consuming or expensive to collect.

425 Breeding objectives differ from the goals of polygenic risk
426 score predictions for human diseases because the prediction
427 target is not the phenotype of an individual, but its genetic value
428 (Runcie and Cheng 2019). Genetic values quantify the expected
429 phenotype of a plant's offspring, and so exclude impacts of the
430 plant's own microenvironment on its phenotype (Bernardo 2010).
431 Therefore, accurate genetic value prediction requires models
432 that can distinguish between genetic and non-genetic sources of
433 covariation among traits.

434 The MvLMM is considered the gold-standard method for
435 isolating genetic correlations from non-genetic correlations in
436 genetic value prediction (Piepho *et al.* 2007). However, it has
437 rarely been applied in breeding programs because of the com-
438 putational challenges associated with estimating multiple large
439 covariance matrices. With high-throughput phenotype (HTP)
440 data, MvLMMs have only been applied directly to sets of $\approx 2 - 5$
441 traits. Instead, several authors have used a prior round of feature
442 selection or calculated summary statistics of the HTP to gener-
443 ate model inputs rather than using the raw high-dimensional
444 data itself (e.g., Jia and Jannink 2012; Guo *et al.* 2014; Rutkoski
445 *et al.* 2016; Sun *et al.* 2017; Crain *et al.* 2018). Other authors have
446 replaced the MvLMM with a direct regression on the HTP data,
447 using techniques such as factorial regression (van Eeuwijk *et al.*
448 2019), functional regression (Montesinos-López *et al.* 2017), ker-
449 nel regression (Krause *et al.* 2019), and deep learning (Cuevas
450 *et al.* 2019). While straightforward to implement, this condition-
451 ing on the HTP traits creates a form of collider bias which can
452 induce genotype-phenotype associations that do not actually
453 exist and impede genetic value predictions (Runcie and Cheng
454 2019). Alternative methods including IBCF (Juliana *et al.* 2019)
455 and regularized selection indexes (Lopez-Cruz *et al.* 2020) avoid
456 computational complexities of the full MvLMMs, but do not
457 make full use of the trait correlations in the data.

458 MegaLMM, on the other hand, fits a full MvLMM to an arbitrary
459 number of HTP traits and should be more efficient at leveraging
460 high-dimensional genetic correlations while accounting for non-
461 genetic sources of covariance, particularly for datasets when
462 HTP traits and focal performance traits are measured on the
463 same plants. Non-genetic correlations will be less important
464 on datasets where these sets of traits are measured on different
465 plots. At least in the wheat breeding trial datasets we exam-
466 ined, the benefit of multi-trait modeling was much greater when
467 traits were partially observed on each individual than when sec-
468 ondary traits were only observed in the training partition. This
469 is expected theoretically and has been demonstrated previously
470 in simulations Runcie and Cheng (2019), but the magnitude of
471 the benefit was particularly dramatic here. This suggests that
472 breeding programs should focus on developing HTP technolo-
473 gies that can measure secondary traits on the target individuals;
474 HTP measurements on training individuals may be less useful
475 for prediction applications. Unlike other methods, including
476 too many traits, or including redundant traits that are highly
477 correlated is unlikely to significantly impact prediction accuracy,
478 reducing the need to carefully choose which traits to include
479 and which to exclude *a priori*; MegaLMM allows users to simply
480 include all traits they have at once.

481 **Applicability to multi-environment trial data**

482 The analysis of multi-environment trials provides a separate set
483 of computational and statistical challenges for plant breeders.
484 Multi-environment trials (METs) are necessary because gene-
485 environment interactions (GEIs) often prevent the same variety
486 from performing best in all locations where a crop is grown
487 (Piepho *et al.* 2007). However, METs are expensive and logis-
488 tically difficult. Genomic predictions in METs could reduce
489 the need to test every variety in every environment, allowing
490 smaller individual trials (Heffner *et al.* 2009).

491 GEIs can be modeled in two ways: (i) as changes in variety
492 effects on the same trait across environments (i.e., variety-by-
493 environment interactions), or (ii) as a set of genetically correlated
494 traits, with each trait-environment combination considered as a
495 different phenotype (Piepho *et al.* 2007). When formulated with
496 linear mixed models and random genetic effects, these two ap-
497 proaches are mathematically equivalent. Traditionally, the most
498 common model for analyzing METs has been the AMMI model
499 in which the genetic effects of each variety in each environment
500 are modeled using a set of products between genetic and en-
501 vironmental vectors (Gauch 1988). AMMI models are used to
502 rank genotypes in different environments and to identify envi-
503 ronmental clusters with similar rankings of varieties. However,
504 AMMI models cannot easily incorporate marker data. When
505 genetic values are treated as random effects, AMMI models be-
506 comes factor models (generally called factor analytic models in
507 this literature) (e.g. Piepho 1998; Smith *et al.* 2001), and can in-
508 incorporate genetic marker data (e.g. Jarquín *et al.* 2014). MegaLMM
509 extends this factor-analytic method for analyzing METs, making
510 the methods robust for METs with hundreds or more individual
511 trials.

512 A limitation of the AMMI factor-analytic approach to analyz-
513 ing METs is that there is no mechanism for extending predictions
514 to new environments outside of those already tested. Even large-
515 scale commercial trials cannot test every field a farmer might use.
516 Several authors have proposed using environmental covariates
517 (ECs) to model environmental similarity in METs and predict
518 GEIs for novel environments (e.g., Jarquín *et al.* 2014; Malosetti
519 *et al.* 2016; Rincent *et al.* 2019). These approaches all involve re-
520 gressions of genetic variation on the ECs, and so, if relevant ECs
521 are missing or the relationship between variety plasticity and
522 ECs is non-linear, these models will under-fit the GEIs. Neverthe-
523 less, these approaches are promising and have been successfully
524 applied to large METs (e.g. Jarquín *et al.* 2014). MegaLMM cannot
525 currently incorporate ECs to predict novel environments. How-
526 ever, a possible extension could involve replacing the *iid* prior on
527 the elements of the factor loadings matrix with a regression on
528 the ECs. This hybrid of ECs and a full MvLMM could leverage
529 the strengths of both approaches.

530 **Model limitations**

531 While MegaLMM works well across a wide range of applications in
532 breeding programs, our approach does have some limitations.

533 First, since MegaLMM is built on the Grid-LMM framework for
534 efficient likelihood calculations (Runcie and Crawford 2019), it
535 does not scale well to large numbers of observations (in contrast
536 to large numbers of traits), or large numbers of random effects.
537 As the number of observational units increases, MegaLMM's mem-
538 ory requirements increase quadratically because of the require-
539 ment to store sets of pre-calculated inverse-variance matrices.
540 Similarly, for each additional random effect term included in the
541 model, memory requirements increase exponentially. Therefore,

542 we generally limit models to fewer than 10,000 observations and
543 only 1-to-4 random effect terms per trait. There may be oppor-
544 tunities to reduce this memory burden if some of the random
545 effects are low-rank; then these random effects could be updated
546 *on the fly* using efficient routines for low-rank Cholesky updates.
547

548 Second, MegaLMM is inherently a linear model and cannot ef-
549 fectively model trait relationships that are non-linear. Some
550 non-linear relationships between predictor variables (like geno-
551 types) and traits can be modeled through non-linear kernel ma-
552 trices, as we demonstrated with the RKHS application to the
553 Bread Wheat data. However, allowing non-linear relationships
554 among traits is currently beyond the capacity of our software
555 and modeling approach. Extending our mixed effect model on
556 the low-dimensional latent factor space to a non-linear modeling
557 structure like a neural network may be an exciting area for future
558 research. Also, some sets of traits may not have low-rank corre-
559 lation structures that are well-approximated by a factor model.
560 For example, certain auto-regressive dependence structures are
561 low-rank but cannot efficiently be decomposed into a discrete
562 set of factors.

563 Nevertheless, we believe that in its current form, MegaLMM
564 will be useful to a wide range of researchers in quantitative
565 genetics and plant breeding.

566 **Potential extensions**

567 Beyond the examples we show in this work, the scalability
568 and statistical power of MegaLMM can open up new avenues
569 for innovation in genomic prediction applications across the
570 fields of quantitative genetics—both in breeding programs as we
571 have described here and, potentially, in human genetics. Ge-
572 nomic prediction is also used for the calculation of polygenic risk
573 scores for complex human traits and diseases ([The International
574 Schizophrenia Consortium 2009](#)). MegaLMM may help leverage
575 past case histories, survey responses, molecular tests, and the
576 genetic architecture of other correlated traits to provide a more
577 comprehensive multi-trait polygenic risk score (e.g. [Turley et al.
578 2018](#)).

579 We have focused here on simple scalar phenotypes: the ex-
580 pression of a single gene, the total grain yield, and individual
581 measures of agronomic performance. However, many important
582 traits in plants, animals, and humans cannot easily be reduced
583 to a scalar value. Examples include time-series traits such as
584 growth curves ([Campbell et al. 2018](#)), metabolic traits such as
585 the relative concentrations of different families of metabolites
586 ([Chan et al. 2011](#)), and morphological traits such as shape or
587 color ([Demmings et al. 2019](#)). Each of these traits can be decom-
588 posed into vectors of interrelated components, but treating these
589 components as independent prediction targets using existing
590 univariate LMM or low-dimensional MvLMM genomic prediction
591 tools is inefficient because of their statistical dependence.
592 MegaLMM can be adapted to make joint predictions on vectors of
593 hundreds or thousands of correlated trait components, which
594 could be fed into high-dimensional selection indices for efficient
595 selection of these important plant characteristics. In human
596 genetics, MegaLMM may provide a way to derive multi-ethnic
597 polygenic risk scores ([Márquez-Luna et al. 2017](#)) by treating
598 outcomes within each ethnic, geographic, or other stratified pop-
599 ulation group as correlated traits, similar to the analysis of the
600 multi-environment trials above.

601 MegaLMM should be straightforward to extend to more flexi-
602 ble genetic models including the Bayesian Alphabet family of
603 mixture priors on marker effect sizes. These effects can be incor-
604 porated into the parameters \mathbf{B}_{2R} and \mathbf{B}_{2F} by adapting the prior
605 structure. This will be further explored in future manuscripts.

606 Lastly, we have only focused on Gaussian MvLMMs, in which
607 observations are assumed to marginally follow a Gaussian distri-
608 bution. However, many other types of data require more flexible
609 models. It should be possible to extend MegaLMM to the broader
610 family of generalized LMMs. These approaches model the rela-
611 tionships among predictor variables in a latent space, which is
612 then related to the observed data through a link function and
613 an exponential family error distribution. More generally, link-
614 functions could be any non-linear function of multiple parame-
615 ters such as a polynomial or spline basis, or a mechanistic model.
616 In this case, we would model the correlations among model
617 parameters on this link-scale and then use the link-function to
618 relate the latent scale variables to the observed data. Extending
619 MegaLMM to accommodate such generalized LMM structures
620 would require new sampling steps in our MCMC algorithm (see
621 Methods), but we do not see any conceptual challenges with this
622 approach.

623 **Conclusions**

624 MegaLMM is a flexible and powerful framework for the analysis of
625 very high-dimensional datasets in genetics. Multivariate linear
626 mixed models are widely used for analyzing correlated traits,
627 but have been limited to a maximum of a dozen or so traits at
628 a time by the curse of dimensionality. We developed a novel
629 re-parameterization of the MvLMM that allows powerful statis-
630 tical regularization and efficient computation with thousands of
631 traits. When applied to real plant breeding objectives, MegaLMM
632 efficiently leverages information across traits to improve genetic
633 value predictions. Our open-source software package will en-
634 able users to apply and extend this method in many directions,
635 opening up new areas of research and development in breeding
636 programs.

637 **Methods**

638 **Multivariate linear mixed models**

639 Multivariate linear mixed models (MvLMMs) are widely used
640 to model multiple sources of covariance among related observa-
641 tions. Let the $n \times t$ matrix \mathbf{Y} represent observations on t traits for
642 n observational units (i.e., individual plants, plots, or replicates).
643 A general MvLMM takes on the following form

$$644 \mathbf{Y} = \mathbf{X}\mathbf{B} + \mathbf{Z}\mathbf{U} + \mathbf{E} \quad (1)$$

645 where \mathbf{X} is a $n \times b$ matrix of “fixed” effect covariates with effect
646 sizes matrix \mathbf{B} , \mathbf{U} is an $r \times t$ matrix of random effects for each of the
647 t traits, with corresponding random effect design matrix \mathbf{Z} , and
648 \mathbf{E} is a $n \times t$ matrix of residuals for each of the t traits.

649 MegaLMM uses this formulation to accommodate a large num-
650 ber of designs through different specifications of \mathbf{X} and \mathbf{Z} , and
651 different priors on \mathbf{B} , \mathbf{U} and \mathbf{E} . The distinction between “fixed”
652 and “random” effects in Bayesian mixed models is not well-
653 defined because every parameter requires a prior. However, we
654 use the following distinction here: “fixed” effects are covari-
655 ates assigned flat (i.e., infinite variance) priors or priors with
656 independent variances on each coefficient; “random” effects, in
657 contrast, are grouped in sets that can be thought of as (possi-
658 bly correlated) samples from a common population distribution.
659 Generally, “fixed” effects are used to model experimental design
660 terms such as blocks, time, sex, etc, genetic principal compo-
661 nents, or specific genetic markers; while “random” effects are
662 used to model genetic values, spatial variation, or related effects.

An important feature of MegaLMM is that the multiple random effect terms can be included in the model. We specify this as

$$\mathbf{ZU} = \sum_{m=1}^M \mathbf{Z}_m \mathbf{U}_m = [\mathbf{Z}_1, \dots, \mathbf{Z}_M] [\mathbf{U}_1^\top, \dots, \mathbf{U}_M^\top]^\top,$$

where each \mathbf{Z}_m is an $n \times r_m$ design matrix for a set of related parameters with corresponding coefficient matrix \mathbf{U}_m . For example, \mathbf{U}_1 may model additive genetic values for each individual, while \mathbf{U}_2 may model spatial environmental effects for each individual. The distribution of each random effect coefficient matrix is $\mathbf{U}_m \sim \mathcal{N}(\mathbf{0}, \mathbf{K}_m, \mathbf{G}_m)$, where $\mathcal{N}(\mathbf{M}, \mathbf{\Sigma}, \mathbf{\Psi})$ is the matrix normal distribution with mean matrix \mathbf{M} , among-row covariance \mathbf{K}_m and among-column (i.e., among-trait) covariance \mathbf{G}_m . We assume that both \mathbf{Z}_m and \mathbf{K}_m are known, while \mathbf{G}_m is unknown and must be learned from the data. Note that \mathbf{K}_m must be positive semi-definite, while \mathbf{G}_m is positive-definite. The covariance among different coefficient matrices is assumed to be zero.

To complete the specification of the MvLMM, we assign the residual matrix the distribution $\mathbf{E} \sim \mathcal{N}(\mathbf{0}, \mathbf{I}_n, \mathbf{R})$ where \mathbf{I}_n is the $n \times n$ identity matrix and \mathbf{R} is an unknown $t \times t$ positive-definite covariance matrix.

Computational challenges with large multi-trait mixed models

Fitting Eq. (1) is challenging because the columns of \mathbf{U} and \mathbf{E} are correlated. This means that data from individual traits (columns of \mathbf{Y}) cannot be treated independently. Maximum-likelihood approaches for fitting MvLMMs (e.g., MTG2) compute the full (or restricted) likelihood of \mathbf{Y} , which involves calculating the inverse of an $nt \times nt$ matrix many times during model optimization. This is computationally prohibitive when n and/or t are large (Figure 2A). Gibbs samplers (e.g., MCMCglmm) avoid forming and computing the inverse of this extremely large matrix, but still require inverting each of the \mathbf{G}_m and \mathbf{R} matrices repeatedly, which is still prohibitive when t is large. Furthermore, the number of parameters in each \mathbf{G}_m and \mathbf{R} grow with the square of t and quickly get larger than the total number of observations (nt) when t is large. This means that \mathbf{G}_m and \mathbf{R} are not identifiable in many datasets and estimates require strong regularization.

Mixed effect factor model

If both \mathbf{G}_m and \mathbf{R} were diagonal matrices, the t traits would be uncorrelated. Fitting Eq. (1) then could be done in parallel across traits, greatly reducing the computational burden. While we cannot directly de-correlate traits, if we can identify the sources of variation that cause trait correlations, the residuals of each trait on these causal factors will be un-correlated. We circumvent this issue by re-parameterizing Eq. (1) as a factor model, where we introduce a set of un-observed (or latent) factors that account for all sources of correlation among the traits. Conditional on the values of these factors, the model reduces to a set of independent linear mixed models. Our re-parameterized multi-trait mixed effect factor model is

$$\begin{aligned} \mathbf{Y} &= \mathbf{F}\boldsymbol{\Lambda} + \mathbf{X}_1\mathbf{B}_1 + \mathbf{X}_2\mathbf{B}_{2R} + \mathbf{ZU}_R + \mathbf{E}_R \\ \mathbf{F} &= \mathbf{X}_2\mathbf{B}_{2F} + \mathbf{ZU}_F + \mathbf{E}_F \end{aligned} \quad (2)$$

where \mathbf{F} is an $n \times K$ matrix of latent factors, $\boldsymbol{\Lambda}$ is a $K \times t$ factor loadings matrix, $\mathbf{X} = [\mathbf{X}_1, \mathbf{X}_2]$ is a partition of the $n \times b$ fixed effect covariate matrix between the b_1 covariates with improper priors and the $b_2 = b - b_1$ covariates with proper priors, and \mathbf{U}_R and \mathbf{U}_F coefficients matrices are specified as:

$$\begin{aligned} \mathbf{U}_R &= [\mathbf{U}_{R1}^\top, \dots, \mathbf{U}_{RM}^\top]^\top \\ \mathbf{U}_F &= [\mathbf{U}_{F1}^\top, \dots, \mathbf{U}_{FM}^\top]^\top. \end{aligned}$$

The distributions of the random effects are specified as:

$$\begin{aligned} \mathbf{U}_{Rm} &\sim \mathcal{N}(\mathbf{0}, \mathbf{K}_m, \mathbf{\Psi}_{Rm}), & \mathbf{U}_{Fm} &\sim \mathcal{N}(\mathbf{0}, \mathbf{K}_m, \mathbf{\Psi}_{Fm}) \\ \mathbf{E}_R &\sim \mathcal{N}(\mathbf{0}, \mathbf{I}_n, \mathbf{\Psi}_{RE}), & \mathbf{E}_F &\sim \mathcal{N}(\mathbf{0}, \mathbf{I}_n, \mathbf{\Psi}_{FE}) \end{aligned}$$

where $\mathbf{\Psi}_{Rm}$, $\mathbf{\Psi}_{Fm}$, $\mathbf{\Psi}_{RE}$, and $\mathbf{\Psi}_{FE}$ are all diagonal matrices. Diagonal elements of $\mathbf{\Psi}_{Fm}$ and $\mathbf{\Psi}_{FE}$ are non-negative, while diagonal elements of $\mathbf{\Psi}_{Rm}$ and $\mathbf{\Psi}_{RE}$ are strictly positive.

Conditional on \mathbf{F} and $\boldsymbol{\Lambda}$, the variation in each of the t columns of \mathbf{Y} are uncorrelated and can be fitted to the remaining terms independently. Similarly, the K columns of \mathbf{F} are also uncorrelated and can be modeled independently as well. Therefore, we can fit Eq. (2) without requiring calculating the inverses of any $t \times t$ matrices, and many calculations can be done in parallel across different CPU cores.

As long as K is sufficiently large, Eq. (2) is simply a re-parameterization of Eq. (1). To see how Eq. (2) can represent the terms of Eq. (1), let:

$$\begin{aligned} \mathbf{B} &= [\mathbf{B}_1^\top, (\mathbf{B}_{2R} + \mathbf{B}_{2F}\boldsymbol{\Lambda})^\top]^\top \\ \mathbf{U} &= \mathbf{U}_R + \mathbf{U}_F\boldsymbol{\Lambda} \\ \mathbf{E} &= \mathbf{E}_R + \mathbf{E}_F\boldsymbol{\Lambda} \end{aligned}$$

Based on the properties of matrix normal random variables, we can integrate over \mathbf{U}_R , \mathbf{U}_F , \mathbf{E}_R and \mathbf{E}_F to calculate the distributions of each \mathbf{U}_m and \mathbf{E} as:

$$\begin{aligned} \mathbf{U}_m &\sim \mathcal{N}(\mathbf{0}, \mathbf{K}_m, \mathbf{\Psi}_{Rm} + \boldsymbol{\Lambda}^\top \mathbf{\Psi}_{Fm} \boldsymbol{\Lambda}) \\ \mathbf{E} &\sim \mathcal{N}(\mathbf{0}, \mathbf{I}_n, \mathbf{\Psi}_{RE} + \boldsymbol{\Lambda}^\top \mathbf{\Psi}_{FE} \boldsymbol{\Lambda}) \end{aligned}$$

Therefore, each \mathbf{G}_m is re-parameterized as $\mathbf{\Psi}_{Rm} + \boldsymbol{\Lambda}^\top \mathbf{\Psi}_{Fm} \boldsymbol{\Lambda}$ and \mathbf{R} is re-parameterized as $\mathbf{\Psi}_{RE} + \boldsymbol{\Lambda}^\top \mathbf{\Psi}_{FE} \boldsymbol{\Lambda}$, such that all off-diagonal elements of each matrix are controlled by $\boldsymbol{\Lambda}$.

Although these equations appear to imply that our mixed effect factor model constrains \mathbf{B} , \mathbf{U} and \mathbf{E} (and thus each \mathbf{G}_m and \mathbf{R}) to be correlated due to the shared dependence on $\boldsymbol{\Lambda}$, this is not necessarily the case. When any diagonal element of any $\mathbf{\Psi}_{Fx}$ matrix is set to zero, the corresponding row of $\boldsymbol{\Lambda}$ does not contribute to that term. If at least t linearly independent rows of $\boldsymbol{\Lambda}$ contribute to each matrix, then any set of positive-definite matrices can be represented as above. Therefore, we can represent any set of positive-definite matrices \mathbf{G}_m and \mathbf{R} with our model as long as $K \geq t(M+1)$.

Of course, the reason that we parameterize our model in this way is that we do expect some correlation among the genetic and residual covariance matrices. From a statistical perspective, when it is reasonable (given the data) to use the same row of $\boldsymbol{\Lambda}$ for multiple covariance matrices, we can save parameters in the model. From a biological perspective, shared factors provide a biologically realistic explanation for correlations among traits. If we consider the columns of \mathbf{F} to be K traits that simply have not been observed, then it is reasonable to propose that each of these traits is regulated by the same sources of genetic and environmental variation as any of the observed traits.

In Eq. (2), the K latent traits (\mathbf{F}) are the key drivers of all phenotypic co-variation among the t observed traits (\mathbf{Y}). These latent traits may not account for all variation in the observed traits. But, by definition, this residual variation (e.g., measurement errors in each trait) is unique to each trait and uncorrelated with the residual variation in other traits.

Prior parameterization. The intuitive structure of the mixed effect factor model (Eq. (2) and Figure 1) makes prior specification and elicitation easier than for Eq. (1) because we do not need to define prior distributions for very large covariance matrices directly. Instead, priors on the random effect variance components and fixed effect regression coefficients are separable and can be described independently, while priors on trait correlations are specified indirectly as priors on the factor loading matrix Λ .

In MegaLMM, we have chosen functional forms for each prior parameter that balance between interpretability (for accurate prior elicitation), and compatibility with efficient computational approaches. For the variance components, we use the non-parametric discrete prior on variance proportions we previously introduced in GridLMM (Runcie and Crawford 2019) that approximates nearly any joint distribution for multiple random effects. For the factor loadings matrix and matrices of regression coefficients, we use a two-dimensional global-local prior based on the horseshoe prior (Carvalho *et al.* 2010), parameterized in terms of the effective number of non-zero coefficients. For the factor loadings matrix specifically, our prior achieves both regularization and interpretability of the factor traits without having to carefully specify K itself. Full details of each prior distribution are provided in the Supplemental Methods. Table S1 lists the default hyperparameters for each prior used in the analyses reported here and provided as defaults in the MegaLMM R package.

Computational details and posterior inference

We use a carefully constructed MCMC algorithm to draw samples from the posterior distribution of each model parameter. We gain efficiency in both per-iteration computational time and in effective samples per iteration through careful uses of diagonalization, sparse matrix algebra, parallelization, and integration (or partial collapsing). In particular, our algorithm synthesizes and extends several recent innovations in computational approaches to linear mixed models (Runcie and Mukherjee 2013; Zhou and Stephens 2012; Makalic and Schmidt 2016; Runcie and Crawford 2019). Full details of the computational algorithm are provided in the Supplemental Methods.

Data Analyses

We demonstrate MegaLMM using three example datasets.

Scaling performance with gene expression data. To compare the scalability of MegaLMM to other multi-trait mixed model programs, we used a large gene expression dataset of 24,175 genes across 728 *Arabidopsis thaliana* accessions. We downloaded the data from NCBI GEO (Barrett *et al.* 2012) (Huang *et al.* GSE80744) and removed genes with average counts < 10 . We then normalized and variance stabilized the counts using the varianceStabilizingTransformation function from DESeq2 (Love *et al.* 2014). We downloaded a corresponding genomic relationship matrix \mathbf{K} from the 1001 genomes project (Alonso-Blanco *et al.* 2016) and subsetted to the 665 individuals present in both datasets.

We generated datasets of varying sizes from $t = 2$ to $t = 24,175$ genes by randomly sampling. We selected one gene as the “focal” trait in each dataset, masked 50% of its values, fit the model in Eq. (1) using four different representative MvLMM programs to the remaining data, and used the results to predict the genetic values of each masked individual for this “focal” gene. Prediction accuracies were estimated as $\rho_g = \text{cor}_g(\hat{\mathbf{u}}, \mathbf{y}) \sqrt{h^2(\hat{\mathbf{u}})}$, where cor_g is the estimated genetic correlation evaluated in the

testing lines only, and $h^2(\hat{\mathbf{u}})$ is the heritability of the predictor $\hat{\mathbf{u}}$ estimated using a univariate LMM (Thompson and Meyer 1986; Lopez-Cruz *et al.* 2020). The simpler Pearson’s correlation estimate of prediction accuracy is not valid in these data because all genes were measured together in the same sample, and therefore some correlation among genes is caused by non-genetic factors (Runcie and Cheng 2019). The four MvLMM predicton methods were:

1. MTG2 (Lee and van der Werf 2016): a restricted maximum-likelihood method written in fortran. We pre-calculated the eigenvalue decomposition for \mathbf{K} , thus this additional time is not included in the results. MTG2 does not work well with a high percentage of missing data, so genetic value predictions were made with the two-step approach from Runcie and Cheng (2019) which involves estimating model parameters only from the individuals with complete observations, and then incorporating secondary trait values of the new individuals in the second step.
2. MCMCglmm (Hadfield 2010): a Bayesian MCMC algorithm largely written in C++. We used “default” priors for \mathbf{R} and \mathbf{G} with diagonal means and $\nu = p$, and ran a single MCMC chain for 7000 iterations, discarding the first 5000 samples as burnin. To speed up calculations (and make the timing results more comparable with the MegaLMM algorithm), we rotated the input data by pre-multiplying by the eigenvectors of \mathbf{K} so that the input relationship matrix was diagonal. Since this matrix rotation is only possible with complete data, we again used the two-step multi-trait prediction approach (Runcie and Cheng 2019).
3. phenix (Dahl *et al.* 2016): a variational Bayes algorithm written in R that uses a low-rank representation of \mathbf{G} but a full-rank prior for \mathbf{R} . We set the maximum number of factors to $p/4$ and used the eigendecomposition of \mathbf{K} as the input. Again, we excluded this calculation from the time estimates.
4. MegaLMM: we ran MegaLMM using “default priors” with $K = \min(n/4, p/2)$ and collected 6000 MCMC samples, discarding the first 5000 as burnin. We excluded the preparatory calculations, only including the MCMC iterations in the time calculations. For small datasets, these calculations were significant, but were a minuscule part of the analyses of larger datasets.

Each method was run 20 times on different randomly sampled datasets. For the two MCMC methods, we estimated the effective sample size of each element of \mathbf{U} using the `ess_bulk` function of the `rstan` package (Stan Development Team 2019), and used this to estimate the time necessary for the effective sample size to be at least 1000 for 90% of the u_{ij} . We ran MTG2 and MCMCglmm for datasets up to $t = 64$ because computational times were prohibitively long for larger datasets. We linearly extrapolated the (log) computational times for these methods out to $t = 512$ for comparisons. phenix fails when $t \geq n$, so this method is limited to $t < 665$ in this dataset.

To assess the accuracy of each method for estimating genetic and non-genetic covariances, we generated new datasets with 128 genes by calculating empirical correlation matrices for \mathbf{G} and \mathbf{R} from two separate samples of 128 genes from the full expression dataset, and then generating genetic and residual values for 128 traits from multivariate normal distributions based on these

correlation matrices. For each trait, we converted the correlation matrices into covariance matrices by sampling an independent heritability value for each trait between 0.1 and 0.8. We then estimated the genetic and residual covariance matrices for subsets of these simulated datasets using each of the four above methods. In this example, we found that setting K larger ($2p$) gave better results, probably because the \mathbf{G} and \mathbf{R} matrices were largely uncorrelated and so independent factors were needed to model the two sets of covariances. Accuracy was reported as the Pearson correlation between the estimated covariance parameters and the true covariance parameters (excluding the variance parameters on the diagonal).

Wheat yield prediction using hyperspectral data. We used data from a bread wheat breeding trial to demonstrate how MegaLMM can leverage “secondary” traits from high-throughput phenotyping technologies to better predict genetic values of a single target trait. We downloaded grain yield and hyperspectral reflectance data from the bread wheat trials at the Campo Experimental Norman E. Borlaug in Ciudad Obregón, México reported in Krause *et al.* (2019) (Mondal *et al.* 2020). We selected the 2014–2015 Optimal Flat site-year for our main analysis because it had among the greatest number of hyperspectral reflectance data points, and Krause *et al.* (2019) reported relatively low predictive accuracy for grain yield in this site-year. Best linear unbiased estimates (BLUEs) and best linear unbiased predictors (BLUPs) of the line means for grain yield (GY) and 62 hyperspectral bands collected at each of 10 time-points during the growing season, and genotype data from 8519 markers were provided for 1,092 lines in this trial. All other trials were analyzed in the analysis presented in Figure S5.

We compared eight methods for predicting the GY trait based on the genetic marker and hyperspectral data. The first five were “standard” methods using state-of-the-art models for genomic prediction. The final three were new models implemented within the MegaLMM framework.

1. GBLUP: implemented using the R package rrBLUP (Endelman 2011), with the genomic relationship matrix \mathbf{K} calculated with the `A.mat` function of rrBLUP as in Endelman and Jannink (2012).
2. Bayesian Lasso (BL): implemented using the R package BGLR (Perez and de los Campos 2014). We first removed markers with $> 50\%$ missing data, and imputed the remaining missing genotypes with the population mean allele frequency. We used the default prior parameters for the Bayesian Lasso in BGLR, and collected 9,000 posterior samples with a thinning rate of 5 after a 5,000 iteration burnin.
3. RKHS: implemented using rrBLUP. We used the same thinned and imputed genotype dataset as for the BL method to calculate a genomic distance matrix (\mathbf{D}). We also used the default `theta.seq` parameter to automatically choose the scale parameter of the Gaussian kernel.
4. HBLUP: implemented using the R package 1me4qt1. This replicates the analysis reported by Krause *et al.* (2019), which uses the GBLUP method but replaces the genomic relationship matrix described above with \mathbf{H} , a hyperspectral reflectance relationship matrix calculated as $\mathbf{H} = \mathbf{S}\mathbf{S}^T/620$, where \mathbf{S} is a matrix of centered and standardized BLUEs of hyperspectral bands from each timepoint.

5. GBLUP+H: implemented in the R package 1me4qt1 (Ziyatdinov *et al.* 2018). This is a two-kernel method, where we use two relationship matrices: \mathbf{K} and \mathbf{H} . This method is analogous to the methods proposed by Krause *et al.* (2019) for leveraging the hyperspectral data in prediction; however, those authors only used two-kernel methods for $G \times E$ prediction across site-years. Since 1me4qt1 does not predict random effects for un-measured observations, we formed predictions as: $\mathbf{K}_{no}\mathbf{K}_{oo}^{-1}\hat{\mathbf{u}}_{ko} + \mathbf{H}_{no}\mathbf{H}_{oo}^{-1}\hat{\mathbf{u}}_{ho}$ where \mathbf{K}_{no} is the $n_n \times n_o$ quadrant of \mathbf{K} specifying the genomic relationships among the n_n “new” un-observed lines, \mathbf{K}_{oo} is the $n_o \times n_o$ quadrant of \mathbf{K} specifying the genomic relationships among the “old” observed lines, $\hat{\mathbf{u}}_{ko}$ is the vector of BLUPs for the genomic random effect, and \mathbf{H}_{no} , \mathbf{H}_{oo} and $\hat{\mathbf{u}}_{ho}$ are similar quantities for the hyperspectral random effect.
6. MegaLMM-GBLUP: we modeled the combined trait data $\mathbf{Y} = [\mathbf{y}, \mathbf{S}]$ with the model specified in Eq. (2) using a single random effect with relationship matrix \mathbf{K} as above, no fixed effects besides an intercept (\mathbf{X} was a column of ones and \mathbf{X}_2 had zero columns). We ran MegaLMM with $K = 100$ factors, “default” priors (see Table S1), and two partitions of the trait data (the first containing grain yield with the masked training set as described below, and the second containing all 620 hyperspectral bands with complete data). We collected 500 posterior samples of the quantity: $\mathbf{u}_1 = \mathbf{u}_{R1} + (\mathbf{U}_F\lambda_1)$ at a thinning rate of 2, discarding the first 1,000 iterations as burn-in.
7. MegaLMM-RKHS: we implemented multi-trait RKHS regression model using the “kernel-averaging” method proposed by de Los Campos *et al.* (2010). We standardized \mathbf{D} based on its mean (squared) value, and placed a uniform prior on the set of scaling factors $h = \{1/5, 1, 5\}$, which we implemented by calculating three corresponding relationship matrices $\mathbf{K}_1, \dots, \mathbf{K}_3$ and by specifying three random effects in Eq. (2). We again used “default” priors, $K = 100$ factors, and treated only the global intercept per-trait as fixed effects. We collected 500 posterior samples of the quantity: $\mathbf{Z}\mathbf{u}_1 = \mathbf{Z}\mathbf{u}_{R1} + \mathbf{Z}(\mathbf{U}_F\lambda_1)$ at a thinning rate of 2, discarding the first 1000 iterations as burn-in.
8. MegaLMM-GBLUP-CV1: we repeated the MegaLMM-GBLUP method above, but this time without partitioning the trait data. Instead, we masked both the grain yield and the 620 hyperspectral band data from the testing set so all lines in the training data had complete data. Predictions of the genetic values were calculated identically to above.

We used cross-validation to evaluate the prediction accuracy of each method. We randomly selected 50% of the lines for model training, 50% for testing, and masked the GY observations for the testing lines. We fit each model to the partially-masked dataset and collected the predictions of GY for the testing lines. We estimated prediction accuracy as $\rho_g = \text{cor}_g(\hat{\mathbf{u}}, \mathbf{y})\sqrt{h^2(\hat{\mathbf{u}})}$ because the hyperspectral reflectance data were collected on the same plots as the GY data and therefore non-genetic (i.e., microenvironmental) factors that affect both reflectance and yield may induce non-genetic correlations among traits (Runcie and Cheng 2019). BLUPs were used as the predictand except in the 2016-17 year when the BLUPs were poorly correlated with the BLUEs suggesting data quality issues. We used a 50-50 training-testing split of the data to ensure that cor_g could be estimated accu-

964 rately in the testing partition. This cross-validation algorithm 1020
965 was repeated 20 times with different random partitions. 1021

966 **Maize trait imputation in multi-environment trials.** We used data 1022
967 on maize hybrids from the Genomes-To-Fields Initiative experiments 1023
968 to demonstrate how MegaLMM can leverage genetic correlations 1024
969 across locations in multi-environment trials. We downloaded 1025
970 the agronomic data from the 2014-2017 field seasons 1026
971 from the CyVerse data repository (McFarland *et al.* 2020) and 1027
972 corresponding genomic data. We used TASSEL5 (Bradbury *et al.* 1028
973 2007) to build a kinship matrix for each hybrid genotype using 1029
974 the CenteredIBS routine. 1030

975 A total of 2012 non-check hybrids with phenotype and 1031
976 genotype data from 108 trials (i.e., site-years) were available. 1032
977 We selected four representative agronomic traits: plant height 1033
978 (cm), grain yield (bushels/acre), days-to-silking (days), and the 1034
979 anthesis-silking interval (ASI, days). For each trait in each site- 1035
980 year, we calculated BLUPs for all observed genotypes using the 1036
981 R package lme4 (Bates *et al.* 2015) with Rep and Block:Rep as 1037
982 fixed effects to account for the experimental design in each field, 1038
983 and formed them into 2012×108 BLUP matrices for each trait. 1039
984 We then dropped site-years where the BLUP variance was zero, 1040
985 or which had fewer than 50 tested lines. On average $\approx 12\%$ of 1041
986 hybrid-site-year combinations were observed across each of the 1042
987 four BLUP matrices. We then used four methods to predict the 1043
988 BLUPs of hybrids that were not grown in each trial: 1044

989 1. GBLUP (univariate): missing values were imputed sepa- 1045
990 rately for each site:year using the `mixed.solve` function of 1046
991 the `rrBLUP` package. 1047

992 2. GBLUP (env BLUPs): genetic values for each hybrid were 1048
993 assumed to be constant across all site-years. We estimated 1049
994 these in two steps. In the first step, we estimated hybrid 1050
995 main effects treating lines as independent random effects 1051
996 using `lme4`, with `site:year` included as a fixed effect. In 1052
997 the second step, we estimated genetic values using the 1053
998 `mixed.solve` function of the `rrBLUP` package. 1054

999 3. phenix: we used `phenix` to impute missing observations in 1055
1000 \mathbf{Y} using \mathbf{K} as a relationship matrix. 1056

1001 4. MegaLMM: we fit the model specified in Eq. (2) to the full 1057
1002 matrix \mathbf{Y} , with $K = 50$ factors and “default”. Here, we 1058
1003 partitioned \mathbf{Y} into 4 sets based on year to minimize the 1059
1004 number of missing observations to condition on during the 1060
1005 MCMC. We collected 1000 posterior samples of imputed 1061
1006 values $\tilde{\mathbf{Y}} = \mathbf{X}_1 \mathbf{B}_1 + \mathbf{F} \Lambda + \mathbf{Z} \mathbf{U}_R$ with a thinning rate of 2, 1062
1007 after discarding the first 5000 iterations as burnin. 1063

1008 We estimated prediction accuracy of each method using cross- 1064
1009 validation. For each of 20 replicate cross-validation runs per 1065
1010 model, we randomly masked 20% of the non-missing BLUPs, 1066
1011 and then calculated the Pearson’s correlation between these 1067
1012 “observed” values and the imputed values of each method. 1068
1013 Pearson’s correlation is appropriate as an estimate of genomic 1069
1014 prediction accuracy in this case because different plants were used 1070
1015 in each trial, so there is no non-genetic source of correlation among 1071
1016 site-years that may bias accuracy estimates. 1072

1017 **Declarations**

1018 **Ethics approval and consent to participate**

1019 Not applicable 1073

1020 **Consent for publication**

1021 Not applicable 1074

1022 **Availability of data and materials**

1023 All data used in these analyses were downloaded from the 1024
1024 publicly accessible repositories described above. 1025
1025 Arabidopsis gene expression data was downloaded from the 1026
1026 NCBI GEO accession GSE80744 available at <http://https://www.ncbi.nlm.nih.gov/geo/query/acc.cgi?acc=GSE80744>. 1027
1027 The Arabidopsis kinship matrix was downloaded from 1028
1028 https://1001genomes.org/data/GMI-MPI/releases/v3.1/SNP_matrix_imputed_hdf5/1001_SNP_MATRIX.tar.gz. 1029
1029 The wheat dataset was downloaded from the CIMMYT Re- 1030
1030 search Data & Software Repository Network available at 1031
1031 <http://hdl.handle.net/11529/10548109>. 1032
1032 The maize phenotype data were downloaded from the CyVerse data repository 1033
1033 based on the links described in (McFarland *et al.* 2020). 1034
1034 Genomic data were downloaded from (http://datacommons.cyverse.org/browse/plant/home/shared/commons_repo/curated/Carolyn_Lawrence_Dill_G2F_Nov_2016_V.3/b_2014_gbs_data). 1035
1035 Scripts for running analyses are available in the GitHub 1036
1036 repository: https://github.com/deruncie/MegaLMM_analyses. 1037
1037 The R package for MegaLMM is available here: <https://github.com/deruncie/MegaLMM/tree/v0.9.1> and is licensed 1038
1038 with the Polyform Noncommercial 1.0 license. The specific 1039
1039 versions of the scripts and package codes are archived at 1040
1040 zenodo with DOIs 10.5281/zenodo.4735048 and 10.5281/zenodo.4740662. 1041

1042 **Competing interests**

1043 The authors declare that they have no competing interests 1044

1045 **Funding**

1046 This work is supported by Agriculture and Food Research Initiative grants no. 2020-67013-30904 and 2018-67015-27957 from the 1047
1047 USDA National Institute of Food and Agriculture to DER and HC. DER is also supported by United States Department 1048
1048 of Agriculture (USDA) National Institute of Food and Agriculture (NIFA), Hatch project 1010469. LC is supported by 1049
1049 grants P20GM109035 (COBRE Center for Computational Biology 1050
1050 of Human Disease; PI Rand) and P20GM103645 (COBRE 1051
1051 Center for Central Nervous; PI Sanes) from the NIH NIGMS, 1052
1052 2U10CA180794-06 from the NIH NCI and the Dana Farber Cancer 1053
1053 Institute (PIs Gray and Gatsonis), as well as by an Alfred 1054
1054 P. Sloan Research Fellowship and a David & Lucile Packard 1055
1055 Fellowship for Science and Engineering. 1056

1057 **Authors’ contributions**

1058 DER developed the method, wrote the R package, developed 1059
1059 and ran the analyses, and wrote the paper. JQ edited the 1060
1060 manuscript HC helped develop the method, design the analysis, 1061
1061 and edited the paper LC helped develop the method, design the 1062
1062 analysis, and wrote the paper 1063

1064 **Acknowledgements**

1065 Not applicable 1070

1071 **References**

1072 Alonso-Blanco, C., J. Andrade, C. Becker, F. Bemm, J. Bergelson, 1073
1073 *et al.*, 2016 1,135 genomes reveal the global pattern of 1074
1074 polymorphism in arabidopsis thaliana. *Cell* **166**: 481–491. 1075

1075 Araus, J. L., S. C. Kefauver, M. Zaman-Allah, M. S. Olsen, and 1137
1076 J. E. Cairns, 2018 Translating High-Throughput Phenotyping 1138
1077 into Genetic Gain. *Trends in plant science* **23**: 451–466. 1139

1078 Barrett, T., S. E. Wilhite, P. Ledoux, C. Evangelista, I. F. Kim, 1140
1079 et al., 2012 Ncbi geo: archive for functional genomics data 1141
1080 sets—update. *Nucleic acids research* **41**: D991–D995. 1142

1081 Bates, D., M. Mächler, B. Bolker, and S. Walker, 2015 Fitting 1143
1082 linear mixed-effects models using lme4. *Journal of Statistical 1144*
1083 Software

1084 Software **67**: 1–48. 1145

1085 Bernardo, R., 2010 *Breeding for Quantitative Traits in Plants*. 1146
1086 Stemma Press, second edition. 1147

1087 Bradbury, P. J., Z. Zhang, D. E. Kroon, T. M. Casstevens, Y. Ram- 1148
1088 doss, et al., 2007 Tassel: software for association mapping of 1149
1089 complex traits in diverse samples. *Bioinformatics* **23**: 2633– 1150
1151 2635.

1090 Burgueño, J., G. de los Campos, K. Weigel, and J. Crossa, 2012 1152
1091 Genomic prediction of breeding values when modeling geno- 1153
1092 type × environment interaction using pedigree and dense 1154
1093 molecular markers. *Crop Science* **52**: 707–719. 1155

1094 Bycroft, C., C. Freeman, D. Petkova, G. Band, L. T. Elliott, et al., 1156
1095 2018 The UK Biobank resource with deep phenotyping and 1157
1096 genomic data. *Nature* **562**: 203–209. 1158

1097 Calus, M. P. and R. F. Veerkamp, 2011 Accuracy of multi-trait 1159
1098 genomic selection using different methods. *Genetics Selection 1160*
1099 Evolution

1100 Campbell, M., H. Walia, and G. Morota, 2018 Utilizing random 1162
1101 regression models for genomic prediction of a longitudinal 1163
1102 trait derived from high-throughput phenotyping. *Plant Direct* 1164
1103 **2**: e00080. 1165

1104 Carvalho, C. M., N. G. Polson, and J. G. Scott, 2010 The horseshoe 1166
1105 estimator for sparse signals. *Biometrika* **97**: 465–480. 1167

1106 Chan, E. K. F., H. C. Rowe, J. A. Corwin, B. Joseph, and D. J. 1168
1107 Kliebenstein, 2011 Combining genome-wide association map- 1169
1108 ping and transcriptional networks to identify novel genes 1170
1109 controlling glucosinolates in *Arabidopsis thaliana*. *PLoS Biol- 1171*
1110 ogy

1111 Crain, J., S. Mondal, J. Rutkoski, R. P. Singh, and J. Poland, 2018 1173
1112 Combining High-Throughput Phenotyping and Genomic In- 1174
1113 formation to Increase Prediction and Selection Accuracy in 1175
1114 Wheat Breeding. - PubMed - NCBI. *The plant genome* **11**: 1176
1115 1–14. 1177

1116 Cuevas, J., O. Montesinos-López, P. Juliana, C. Guzman, P. Pérez- 1178
1117 Rodríguez, et al., 2019 Deep Kernel for Genomic and Near 1179
1118 Infrared Predictions in Multi-environment Breeding Trials. 1180
1119 *G3: Genes | Genomes | Genetics* **9**: 2913–2924. 1181

1120 Dahl, A., V. Iotchkova, A. Baud, Å. Johansson, U. Gyllensten, 1182
1121 et al., 2016 A multiple-phenotype imputation method for ge- 1183
1122 netic studies. *Nature Genetics* **48**: 466–472. 1184

1123 de Los Campos, G. and D. Gianola, 2007 Factor analysis models 1185
1124 for structuring covariance matrices of additive genetic effects: 1186
1125 a Bayesian implementation. *Genetics Selection Evolution* **39**: 1187
1126 481–494. 1188

1127 de Los Campos, G., D. Gianola, G. J. M. Rosa, K. A. Weigel, and 1189
1128 J. Crossa, 2010 Semi-parametric genomic-enabled prediction 1190
1129 of genetic values using reproducing kernel Hilbert spaces 1191
1130 methods. *Genetics Research* **92**: 295–308. 1192

1131 Demmings, E. M., B. R. Williams, C.-R. Lee, P. Barba, S. Yang, 1193
1132 et al., 2019 Quantitative Trait Locus Analysis of Leaf Morphol- 1194
1133 ogy Indicates Conserved Shape Loci in Grapevine. *Frontiers 1195*
1134 in plant science

1135 Endelman, J. B., 2011 Ridge regression and other kernels for 1197
1136 genomic selection with r package rrblup. *Plant Genome* **4**: 1198
250–255.

Endelman, J. B. and J.-L. Jannink, 2012 Shrinkage Es- 1199
1200 timation of the Realized Relationship Matrix. *G3: Genes | Genomes | Genetics* **2**: 1405–1413.

Gauch, H. G., 1988 Model Selection and Validation for Yield 1201 Trials with Interaction. *Biometrics* **44**: 705–715.

Gilmour, A. R., 2007 Mixed model regression mapping for QTL 1202 detection in experimental crosses. *Computational Statistics & 1203 Data Analysis* **51**: 3749–3764.

GTEx Consortium, 2017 Genetic effects on gene expression 1204
1205 across human tissues. *Nature* **550**: 204–213.

Guo, G., F. Zhao, Y. Wang, Y. Zhang, L. Du, et al., 2014 Com- 1206
1207 parison of single-trait and multiple-trait genomic prediction 1208
1209 models. *BMC Genetics* **15**: 30.

Hadfield, J. D., 2010 MCMC methods for multi-response gen- 1210
1211 eralized linear mixed models: the MCMCglmm R package. 1212
1213 *Journal of Statistical Software*.

Hayes, B. J., P. J. Bowman, A. C. Chamberlain, K. Verbyla, and 1214
1215 M. E. Goddard, 2009 Accuracy of genomic breeding values 1216
1217 in multi-breed dairy cattle populations. *Genetics Selection 1218*
1219 Evolution

Heffner, E. L., M. E. Sorrells, and J.-L. Jannink, 2009 Genomic 1220
1221 Selection for Crop Improvement. *Crop Science* **49**: 1–12.

Henderson, C. R. and R. L. Quaas, 1976 Multiple Trait Evaluation 1222
1223 Using Relatives' Records. *Journal of animal science* **43**: 1188– 1224
1225 1197.

Huang, S., T. Kawakatsu, F. Jupe, R. Schmitz, M. Urich, et al., 1226
1227 GSE80744 Epigenomic and genome structural diversity 1228
1229 in a worldwide collection of *arabidopsis thaliana*. Available 1230
1231 at <http://https://www.ncbi.nlm.nih.gov/geo/query/acc.cgi?acc=GSE80744>.

Jarquín, D., J. Crossa, X. Lacaze, P. Du Cheyron, J. Daucourt, et al., 1232
1233 2014 A reaction norm model for genomic selection using high- 1234
1235 dimensional genomic and environmental data. *Theoretical and 1236
1237 Applied Genetics* **127**: 595–607.

Jia, Y. and J.-L. Jannink, 2012 Multiple-Trait Genomic Selection 1238
1239 Methods Increase Genetic Value Prediction Accuracy. *Genetics 1240*
1241 **192**: 1513–1522.

Johnstone, I. M. and D. M. Titterington, 2009 Statistical chal- 1242
1243 lenges of high-dimensional data. *Philosophical transactions. Series A, Mathematical, physical, and engineering sciences* 1244
1245 **367**: 4237–4253.

Juliana, P., O. A. Montesinos-López, J. Crossa, S. Mondal, L. González-Pérez, et al., 2019 Integrating genomic-enabled 1246
1247 prediction and high-throughput phenotyping in breeding for 1248
1249 climate-resilient bread wheat. *Theoretical and Applied Genetics 1250*
1251 **132**: 177–194.

Kang, H. M., N. A. Zaitlen, C. M. Wade, A. Kirby, D. Heckerman, 1252
1253 et al., 2008 Efficient control of population structure in model 1254
1255 organism association mapping. *Genetics* **178**: 1709–1723.

Koltes, J. E., J. B. Cole, R. Clemmens, R. N. Dilger, L. M. Kramer, 1256
1257 et al., 2019 A vision for development and utilization of high- 1258
1259 throughput phenotyping and big data analytics in livestock. 1260
1261 *Frontiers in Genetics* **10**: 1197.

Krause, M. R., L. González-Pérez, J. Crossa, P. Pérez-Rodríguez, O. Montesinos-López, et al., 2019 Hyperspectral Reflectance- 1262
1263 Derived Relationship Matrices for Genomic Prediction of 1264
1264 Grain Yield in Wheat. *G3: Genes | Genomes | Genetics* **9**: 1231– 1265
1266 1247.

Lee, S. H. and J. H. J. van der Werf, 2016 MTG2: an efficient 1267
1268 algorithm for multivariate linear mixed model analysis based 1269
1270 on genomic information. *Bioinformatics* **32**: 1420–1422.

1199 Lippert, C., J. Listgarten, Y. Liu, C. M. Kadie, R. I. Davidson, *et al.*, 1261
1200 2011 FaST linear mixed models for genome-wide association 1262
1201 studies. *Nature methods* **8**: 833–835. 1263

1202 Loh, P.-R., G. Tucker, B. K. Bulik-Sullivan, B. J. Vilhjálmsdóttir, 1264
1203 H. K. Finucane, *et al.*, 2015 Efficient Bayesian mixed-model 1265
1204 analysis increases association power in large cohorts. *Nature* 1266
1205 *Genetics* **47**: 284–290. 1267

1206 Lopez-Cruz, M., E. Olson, G. Rovere, J. Crossa, S. Dreisigacker, 1268
1207 *et al.*, 2020 Regularized selection indices for breeding value 1269
1208 prediction using hyper-spectral image data. *bioRxiv* **125**: 1270
1209 625251. 1271

1210 Love, M. I., W. Huber, and S. Anders, 2014 Moderated estimation 1272
1211 of fold change and dispersion for rna-seq data with deseq2. 1273
1212 *Genome Biology* **15**: 550. 1274

1213 Makalic, E. and D. F. Schmidt, 2016 A Simple Sampler for the 1275
1214 Horseshoe Estimator. *IEEE Signal Processing Letters* **23**: 179– 1276
1215 182. 1277

1216 Malosetti, M., D. Bustos-Korts, M. P. Boer, and F. A. van Eeuwijk, 1278
1217 2016 Predicting Responses in Multiple Environments: Issues 1279
1218 in Relation to Genotype \times Environment Interactions. *Crop* 1280
1219 *Science* **56**: 2210–2222. 1281

1220 Márquez-Luna, C., P.-R. Loh, S. A. T. . D. S. Consortium, T. S. T. 1282
1221 . D. Consortium, and A. L. Price, 2017 Multi-ethnic polygenic 1283
1222 risk scores improve risk prediction in diverse populations. 1284
1223 *Genetic Epidemiology* **41**: 811–823. 1285

1224 McFarland, B. A., N. AlKhalifah, M. Bohn, J. Bubert, E. S. Buckler, 1286
1225 *et al.*, 2020 Maize genomes to fields (G2F): 2014–2017 field 1287
1226 seasons: genotype, phenotype, climatic, soil, and inbred ear 1288
1227 image datasets. *BMC Research Notes* **13**: 1–6. 1289

1228 Meuwissen, T. H., B. J. Hayes, and M. E. Goddard, 2001 Prediction 1290
1229 of total genetic value using genome-wide dense marker 1291
1230 maps. *Genetics* **157**: 1819–1829. 1292

1231 Meyer, K., 2007 Multivariate analyses of carcass traits for Angus 1293
1232 cattle fitting reduced rank and factor analytic models. *Journal* 1294
1233 of *Animal Breeding Genetics* **124**: 50–64. 1295

1234 Mondal, S., M. Krause, P. Juliana, J. Poland, S. Dreisigacker, *et al.*, 1296
1235 2020 Use of hyperspectral reflectance-derived relationship 1297
1236 matrices for genomic prediction of grain yield in wheat - data 1298
1237 for publication. 1299

1238 Montesinos-López, A., O. A. Montesinos-López, J. Cuevas, 1300
1239 W. A. Mata-López, J. Burgueño, *et al.*, 2017 Genomic Bayesian 1301
1240 functional regression models with interactions for predicting 1302
1241 wheat grain yield using hyper-spectral image data. *Plant* 1303
1242 *Methods* **13**: 1. 1304

1243 Neethirajan, S., 2017 Recent advances in wearable sensors for 1305
1244 animal health management. *Sensing and Bio-Sensing Research* 1306
1245 **12**: 15–29. 1307

1246 Park, T. and G. Casella, 2013 The Bayesian Lasso. *Journal Of The* 1308
1247 *American Statistical Association* **103**: 681–686. 1309

1248 Perez, P. and G. de los Campos, 2014 Genome-wide regression 1310
1249 and prediction with the bglr statistical package. *Genetics* **198**: 1311
1250 483–495. 1312

1251 Piepho, H.-P., 1998 Empirical best linear unbiased prediction in 1313
1252 cultivar trials using factor-analytic variance-covariance struc- 1314
1253 tures. *Theoretical and Applied Genetics* **97**: 195–201. 1315

1254 Piepho, H. P. and J. Möhring, 2005 Best Linear Unbiased Prediction 1316
1255 of Cultivar Effects for Subdivided Target Regions. *Crop* 1317
1256 *Science* **45**: 1151–1159. 1318

1257 Piepho, H. P., J. Möhring, A. E. Melchinger, and A. Büchse, 2007 1319
1258 BLUP for phenotypic selection in plant breeding and variety 1320
1259 testing. *Euphytica* **161**: 209–228. 1321

1260 Rincent, R., M. Malosetti, B. Ababaei, G. Touzy, A. Mini, *et al.*, 1322
1261 2019 Using crop growth model stress covariates and AMMI 1323
1262 decomposition to better predict genotype-by-environment interactions. *TAG Theoretical and applied genetics Theoretische* 1324
1263 *und angewandte Genetik* **132**: 3399–3411. 1325

1264 Runcie, D. and H. Cheng, 2019 Pitfalls and remedies for cross 1326
1265 validation with multi-trait genomic prediction methods. *G3: Genes, Genomes, Genetics* **9**: 3727–3741. 1327

1266 Runcie, D. and L. Crawford, 2019 Fast and flexible linear 1328
1267 mixed models for genome-wide genetics. *PLOS Genetics* **15**: 1329
1268 e1007978. 1330

1269 Runcie, D. and S. Mukherjee, 2013 Dissecting High-Dimensional 1331
1270 Phenotypes with Bayesian Sparse Factor Analysis of Genetic 1332
1271 Covariance Matrices. *Genetics* **194**: 753–767. 1333

1272 Rutkoski, J., J. Poland, S. Mondal, E. Autrique, L. G. Pérez, 1334
1273 *et al.*, 2016 Canopy Temperature and Vegetation Indices from 1335
1274 High-Throughput Phenotyping Improve Accuracy of Pedigree 1336
1275 and Genomic Selection for Grain Yield in Wheat. *G3: Genes | Genomes | Genetics* **6**: 2799–2808. 1337

1276 Schrag, T. A., M. Westhues, W. Schipprack, F. Seifert, A. Thiemann, *et al.*, 2018 Beyond Genomic Prediction: Combining 1338
1277 Different Types of omics Data Can Improve Prediction of Hybrid 1339
1278 Performance in Maize. *Genetics p. genetics*.300374.2017. 1340

1279 Smith, A., B. Cullis, and R. Thompson, 2001 Analyzing Variety 1341
1280 by Environment Data Using Multiplicative Mixed Models and 1342
1281 Adjustments for Spatial Field Trend. *Biometrics* **57**: 1138–1147. 1343

1282 Stan Development Team, 2019 RStan: the R interface to Stan. R 1344
1283 package version 2.19.2. 1345

1284 Sun, J., J. E. Rutkoski, J. A. Poland, J. Crossa, J. L. Jannink, *et al.*, 1346
1285 2017 Multitrait, Random Regression, or Simple Repeatability 1347
1286 Model in High-Throughput Phenotyping Data Improve Genomic 1348
1287 Prediction for Wheat Grain Yield. *The plant genome* **10**: 0. 1349

1288 The International Schizophrenia Consortium, 2009 Common 1350
1289 polygenic variation contributes to risk of schizophrenia and 1351
1290 bipolar disorder. *Nature* **460**: 748–752. 1352

1291 Thompson, R. and K. Meyer, 1986 A review of theoretical aspects 1353
1292 in the estimation of breeding values for multi-trait selection. 1354
1293 *Livestock Production Science* **15**: 299–313. 1355

1294 Turley, P., R. K. Walters, O. Maghzian, A. Okbay, J. J. Lee, *et al.*, 1356
1295 2018 Multi-trait analysis of genome-wide association summary 1357
1296 statistics using mtag. *Nature genetics* **50**: 229–237. 1358

1297 van Eeuwijk, F. A., D. Bustos-Korts, E. J. Millet, M. P. Boer, 1359
1298 W. Kruijzer, *et al.*, 2019 Modelling strategies for assessing and 1360
1299 increasing the effectiveness of new phenotyping techniques 1361
1300 in plant breeding. *Plant Science* **282**: 23–39. 1362

1301 Zhou, X. and M. Stephens, 2012 Genome-wide efficient mixed- 1363
1302 model analysis for association studies. *Nature Genetics* **44**: 1364
1303 821–824. 1365

1304 Zhou, X. and M. Stephens, 2014 Efficient multivariate linear 1366
1305 mixed model algorithms for genome-wide association studies. 1367
1306 *Nature methods* **11**: 407–409. 1368

1307 Ziyatdinov, A., M. Vazquez-Santiago, H. Brunel, A. Martinez- 1369
1308 Perez, H. Aschard, *et al.*, 2018 lme4qtl: linear mixed models 1370
1309 with flexible covariance structure for genetic studies of related 1371
1310 individuals. *BMC Bioinformatics p. btw080*. 1372